AN ABSTRACT OF THE THESIS OF

Logan L. Lewis for the degree of Master of Science in Geology presented on March 10, 2023.

Title: Measuring Sediment Transport Rates Using Tracer Gravel and RFID Technology.

Abstract approved: _____

Stephen T. Lancaster

Rates of sediment transport were determined using tracer gravel and a RFID antenna array at Oak Creek (Oregon) to compare a new method with an existing transport relation created from data previously collected in the same study reach. Close to 3,000 tracers were deployed throughout the study reach and were composed of particles from four different class sizes, including 11–16 mm, 16–32 mm, 32–64 mm, and 64–101.5 mm. Tracer positions were monitored between 2016–2022 using three antennas, stretching across the stream channel, on the bed of the stream and a handheld antenna was used to locate tracer positions between antennas and downstream of the array. Transport rates were calculated from inter-arrival times of pairs of tracers moving in and out of the readable range of an antenna.

Results showed that for any given discharge, transport rates for tracer gravel were lower than what was expected from the other transport relation for the reach. Specifically, the smaller two size classes displayed transport rates lower by an order of magnitude or greater than what was expected, while the larger two sizes classes produced rates inside of an order of magnitude lower. Several problems with the methodology presented themselves over the course of data collection but did not affect the quality of the data gathered. Results from this study build on a

plethora of previous work using tracer particles over the last few decades and this methodology has the potential to be used more widely and on larger stream systems.

Measuring Sediment Transport Rates Using Tracer Gravel and RFID Technology

by
Logan L. Lewis

A THESIS

submitted to

Oregon State University

in partial fulfillment of
the requirements for the
degree of

Master of Science

Presented March 10, 2023
Commencement June 2023

Master of Science thesis of Logan L. Lewis presented on March 10, 2023

APPROVED:

Major Professor, representing Geology

Dean of the College of Earth, Ocean, and Atmospheric Sciences

Dean of the Graduate School

I understand that my thesis will become part of the permanent collection of Oregon State University libraries. My signature below authorizes release of my thesis to any reader upon request.

Logan L. Lewis, Author

ACKNOWLEDGEMENTS

My appreciation goes to Dr. Stephen T. Lancaster for the idea behind the research topic and his guidance in the field, lab, and help with putting this thesis together. Much appreciation also goes to Jon Sanfilippo, a previous student of Dr. Lancaster, who created and modified most of the field equipment used in the study. Additionally, many current and previous OSU undergraduate research assistants and volunteers who helped in the lab and field need to be acknowledged, including Morgan Tholl, Daniel Azzopardi, Liam Reardon, Sophia Cipriano, Brandon Larrabee, Nathaniel Edmonds, and Jordon Dillahunty. Vince Transquilli (ODFW), Dana Warren (OSU DFW), and Nate Bradley (USBR) also provided advice and incites for deploying tracers and utilizing RFID technology. I am also indebted to Dr. Catalina Segura and her current/previous students, Scott Katz, Sami Cargill, Sandra Villamizar, and Zach Perry, who collected the data required to develop the stage-discharge relationship for Oak Creek. RFID equipment for this study was supplied by Dr. Joel Johnson, David Leer, and Oregon RFID.

TABLE OF CONTENTS

LIST OF FIGURES

LIST OF FIGURES (Continued)

LIST OF TABLES

1. Introduction

In ideal or controlled conditions, such as a flume or modified stream channel, rates of gravel transport vary with shear stress and bed texture, and in such experimental settings, bed forms are typically absent and flow conditions are uniform and steady, so variations in transport rate can be adequately characterized and predicted (Einstein, 1950; Meyer-Peter and Muller, 1948; Parker at al., 1982). In the field setting, flow variation and channel geometry complicate the determination of relationships between discharge and gravel transport rates, especially in forested mountain streams which are characterized by large amounts of in-stream debris. Despite the plethora of available bedload transport relations, considerable debate has persisted due to variability of transport in gravel-bed streams.

Over the past few decades, a variety of methods using tracer particles have been used to evaluate mechanisms of sediment transport (Bradley and Tucker, 2012; Bradley, 2017; Hubbell and Sayre, 1964; Lamarre, Macvicar, and Roy, 2005; Lamarre and Roy, 2008; Liébault et al., 2012; Phillips, Martin, and Jerolmack, 2013; Sayre and Hubbell, 1965). While tracer studies have provided valuable insights, it is still unclear whether the data collected provides the necessary measurements needed for calculating sediment transport rates. Additionally, tracer studies typically lack the means to determine exact timing of transport with finer resolution than a particular peak storm event, for which specific hydraulic data is also usually lacking. Recent deployments of RFID instrumentation have proven successful in monitoring specific movements of wildlife and has proceeded to be utilized by sediment transport researchers, where both place-and-relocate methodology and real-time movement monitoring of gravel using antennas has

proven effective (Olinde and Johnson, 2013; Olinde and Johnson 2015). Still, recent tracer studies have not been able to specifically measure rates of sediment with the continued improvement of methodologies. Therefore, it seems that there is a need for a study with a modest goal of recording field-based bedload transport rates with high resolution in space and time, and pertinent to mountain streams. At Oak Creek (Oregon), bedload transport data has already been gathered and utilized to develop well-known sediment transport models and modifications to those models (Parker et al, 1982; Parker, 1990; Parker and Klingeman 1982). With that in mind, it appears to be an ideal location for developing and testing new methodologies.

For this study, close to 3,000 gravel tracers embedded with PIT tags were deployed to Oak Creek and monitored using RFID technology. Deployment of tracers and collection of data began in 2016 and continued until 2022, where simple modifications to enhance the system were conducted over the time of data collection. Both a fixed antenna array and handheld antenna were used to monitor and locate tracer positions throughout the study reach. Transport rates were developed using inter-arrival times between tracers reaching either the upstream or downstream limit of an antenna's readable range. The research method was based on the idea the movement of tracers deployed in a reach of a stream can be studied and used to estimate bedload transport. Continuing to advance methods for tracer studies is important for improving the prediction of gravel movement and for enhancing restoration practices.

This study has the following main objectives:

- Use RFID instrumentation to make continuous measurements of sediment transport;

- Evaluate the new method by compare transport rates with an established model from Oak Creek; and
- Leave behind a large database of tracer particle movement that could be utilized in the future for additional purposes.

2. Literature Review

Bedload refers to sediment, such as sand and cobbles, being transported along the stream channel bottom by rolling, sliding, or bouncing, and this process in commonly known as saltation. Coarse particles travel the bed for shorts burst of time and are deposited quickly and stored within a stream channel, in contrast to suspended sediment that move downstream without any intermittent stages of deposition. The time for which coarse material remains stationary within a stream channel varies due to many parameters, including the size, shape, and density of the material. Additionally, relationships between bedload particles, their exposure to flow, and the flow characteristics of streams play a large role in determining how long a particle may remain stationary. Along most streams, it is more probable that coarse material is immobile for substantially longer periods of time than for which it is in motion.

Considerable thought has been devoted to documenting both changes in suspended and bedload transport with rising discharge at a location because forecasting changes is fundamental to determining erosion rates, channel responses to human activities, the transport of contaminants attached to particles, and many other potential problems. For most rivers, the load of suspended sediment at a given site directly increases with discharge, indicating that the movement of sediment in a river is greater at high discharges (Thorne, Bathurst, and Hey, 1987). Fine sediment added to a river during high discharges is derived from the valley slopes of a watershed, stream channel erosion, the stream channel itself, or supplementary inputs from tributary streams. This means that the concentrations of fine-grained sediment hinges on the supply to the river and not necessarily the power of any given flow. Recent studies using

geochemical tracers in fine-grained sediments support the idea that the supply of sediment is more important than the velocity and duration of flow (Collins et al., 1997; Miller at al., 2005; Walling et al., 1999). Not all rivers display the trait of higher suspended sediment loads during high discharge events and Williams (1989) identified relationships existing between suspended sediment concentration and discharge for a given river, including the amount of sediment stored along a channel, distribution of precipitation within a basin, the rate of runoff, and several other traits.

In contrast to suspended sediment, coarse sediment is generally available in amounts larger than a stream can carry and should correlate more closely with the depth and velocity of high flow events. Traditionally, direct measurements for establishing relationships between discharge and bedload transport have been difficult to assess because the amount of sediment passing a stream channel cross-section fluctuates greatly with time, the amount of bedload at a given time varies along different points of a channel cross-section, and handheld and in-stream measuring devices can only sample for short periods of time and often disrupt natural flow (Leopold and Emmett, 1977; Hoey, 1992; Carling at al., 1998). Additionally, data from a wide range of flows are required to build robust relationships between discharge and flow. Due to the difficulties surrounding these measurements, estimates of bedload discharge have primarily been made using empirical models, developed in lab flumes or heavily instrumented sites, that predict the amount of sediment a stream can carry for different channel widths and flow conditions (Einstein, 1950; Meyer-Peter and Muller, 1948; Parker at al., 1982; Recking, 2013a; Yager, et al., 2007). The accuracy of proposed models is difficult to quantify because reliable field-based measurements of bedload transport for a wide range of discharges are scarce, compared to that of flume-base

data. Though the problem of recording field-based bedload transport data seems to be a difficult task, recent technological advances in detecting movement of bedload material using tracer particles has initiated new optimism to the effort (Bradley and Tucker, 2012; Bradley, 2017; Liébault et al., 2012; ; Olinde and Johnson, 2013; Olinde and Johnson 2015; Phillips, Martin, and Jerolmack, 2013).

A continuing problem in the study of sediment transport in gravel-bed streams are the comprehensive description of individual and bulk tracer particle displacements in relation to channel morphology, flow characteristics, and bed texture. Channel morphology and bed-surface composition are forthright outcomes of particle movements and, in turn, place constraints on particle displacement. Detailed descriptions of sediment dispersion in streams are fundamental for understanding and predicting channel stability, changes in bed texture, deviations in sediment mobility, depth of the active layer, aquatic habitat, and overall landscape evolution. Thorough observations of the wide range in movements of tracer particles will improve the characterization of transport in streams and will likely provide the information needed for the modification and development of better predictive models. While the exact methods for tracking large numbers of tracer particles still poses a major limitation on particle tracking efforts, considerable research has been conducted using tracer particles. Even accounting for the previous efforts, many gaps in our knowledge continue to exist. Tracer studies continue to remain at the level of examining basic features of grain movements, such as the frequency of grain displacements, the mode of movement, and the travel speed and distance in relation to specific particle properties and flow characteristics (Hassan and Bradley, 2017). Major gaps in research include partitioning particle storage timescales, relations between burial depth and particle mobility, the roles of mobile and

immobile particles within the active layer, spatial and temporal patterns of bed mobility, and developing reliable sediment transport rates. To account for the described gaps, long-term tracer monitoring studies in a wide range of fluvial environments are required so disparities in knowledge can be filled.

Experiments with tracer particles provides discreet aid for observing the kinematics of gravel movement, so when using a small sample of bed material, tracers can represent the whole bed and provide insights on particle displacement and transport. Tracer studies have the potential to characterize long-term activity of the fluvial system under varying flow, and potentially uncover the influence of channel morphology, bedform, and bed composition on article movement. In general, tracer technology falls into two distinct categories: “active” and “passive” tracers. An active tracer is characterized by a natural or artificial particle that contains a battery-powered radio transmitter that can broadcast to receivers close to the study area. Active tracer particles are initially hindered by the size of the transmitter and battery, so only large particles can be used in the field setting. The major advantage of using active tracers is that transport is observed in real-time and is effectively correlated with changes in a hydrograph during peaks flows. Real-time observations can identify if a tracer is at rest or in motion, additionally, tracer step lengths and resting time can be determined. Studies using active tracers have shown that step lengths are exponential, or gamma distributed, and that resting times are more commonly exponentially distributed (Ergenzinger and Schmidt, 1990; Habersack, 2001; McNamara and Borden, 2004; Schmidt and Ergenzinger, 1992). Nonetheless, active tracers are expensive and restricted by battery life, so the number of tracers in an experiment and the amount of motion captured is over short periods of time.

Passive tracers are usually either fine sediment or gravel that is tagged in some way so that the concentration of tracers on the bed can be measured. Initial tracer experiments deployed sand labeled with radioactive material, allowing for continuous detection of particles at the surface and in the subsurface over large areas over specific intervals of time (Hubbell and Sayre, 1964; Sayre and Hubbell, 1965). For obvious reasons, concerns with introducing radioactive material to stream systems has stopped any additional use of the method to track fine sediment. Therefore, passive tracer methodologies have used gravel-sized particles. Gravel tracers are generally customized so that they are easy to find after they have been transported, such as painted rocks, inserting magnetic or iron parts, and most recently, using passive integrated transponder (PIT) tags. Fish biologists have been using PIT tags to track fish for years, and geomorphologists have adopted the use of PIT tags to monitor gravel movement. Passive tracers are generally cheap and not limited by battery life, making larger deployments of tracers possible and dramatically increasing the time periods for which data can be collected, compared to active tracers. Earlier uses of passive tracers found that the main disadvantages included low recovery rates, degeneration of labels, and the need to dig tracers out of the stream bed to identify them, but recent uses of PIT tags (Bradley and Tucker, 2012; Bradley, 2017; Lamarre, Macvicar, and Roy, 2005; Lamarre and Roy, 2008; Liébault et al., 2012; Olinde and Johnson, 2013; Olinde and Johnson, 2015; Phillips, Martin, and Jerolmack, 2013) have been able to overcome those initial disadvantages. Unfortunately, recovery techniques using PIT tags are limited to wadable streams and are not suitable for large rivers (Liedermann, Tritthart, and Habersack, 2013). Recent addition of RFID antennas with the use of PT tags has the potential to overcome this drawback (Olinde and Johnson, 2013; Olinde and Johnson 2015). Through the wide range of tracer studies,

it is still unclear what method is most useful or if the information collected was enough to effectively measure sediment transport rates. Furthermore, previous tracer studies cannot determine specific times of tracer movement within single peak flow events, for which hydraulic data, such as flow depth, flow velocity and water surface gradient, are typically lacking.

At Oak Creek, a gravel-bed stream in the Oregon Coast Range, sediment transport equations based on reach-averaged shear stress estimates were formulated based on both surface (Parker, 1990) and subsurface (Parker et al., 1982; Parker and Klingeman, 1982) grain size information. These sediment transport equations were developed based on bedload data collected utilizing a vortex sampler taking measurements between 1969 and 1990; data from 1971 were published in the thesis work of Milhous (1973). The bedload sampler was incorporated into a broad-crested weir, which acted as a control for water level and to provide a stage-discharge relationship for the study reach. This dataset using the vortex sampler enabled capturing the total bedload flux of sand to cobble sized particles over a wide range of flows, which resulted in a lower error compared to that of other methods of sampling bedload transport (Parker et al., 1982). Additionally, these formulations used transport data gathered during conditions when the substrate was considered to be broken.

Although the previously mentioned transport relations (Parker et al, 1982; Parker, 1990; Parker and Klingeman 1982), based on Oak Creek data, have been successfully applied to other rivers, Recking (2013b) characterized the variability in transport rate estimates due to uncertainty in input shear stress values using a reach averaged approach. Recent work has helped document the spatial variability of shear stress present throughout Oak Creek (Katz et al., 2018; Monsalve et

al., 2016), in contrast to older models formulated through the reach which have relied on a reach-averaged value. Monsalve et al. (2020) identified a full distribution of shear stress at Oak Creek using two-dimensional flow modeling, rather than a reach-averaged shear stress value for a given flow. From the new model, predicted values of shear stress were 66-79% smaller than the mean shear stress values identified using a depth-slope product. Additionally, the new transport formulation predicts bedload transport rates at a wider range of flows but relies on detailed numerical flow modeling and field measurements, potentially placing limitation on its use in other streams.

Prediction of gravel movement is an important issue for scientists, engineers, and other related managers who are concerned with sediment sources, distribution of transport distance, and how they are related to overall transport rates. These issues have recently been addressed by Furbish et al (2012) and Roseberry et al. (2012), but only with a small number of tracer particles and over short periods of time. Moreover, these studies only address the fate of particles deployed at a single location. It seems likely that the distribution of transport distance is dependent on the location of deployment, as well as conditions downstream and upstream. While these distinctions may seem obvious, they may be crucial to understanding how mitigation and restoration treatments affecting water surface gradients also affect the likely sources of sediment to a site. For example, if in-channel debris reduced the gradient in a given reach enough for the channel to move along the spectrum from detachment, or supply limited, to transport limited in respect to gravel, then gravel will move through the reach at a reduced rate, so the reach will still be able to receive sediment from upstream and supply sediment to downstream reaches, and this condition might be better for salmonid fish, both for spawning and rearing. However, if the stream channel

moves along the spectrum to being threshold limited, the reach will neither receive nor supply gravel at significant rates. Decreases in gravel supply would likely increase fine sediment deposition through a reach and may no longer provide spawning habitat.

It is likely that different limitations apply at different points along a stream with varying quantities of in-channel debris, so, at any given point, the possible upstream areas contributing gravel can decrease as a function its ability to transport material downstream. The recent work of Roseberry et al. (2012) showed that the velocity of particles in motion are not sensitive to transport rate, but the bed material's activity is more sensitive to variations in transport rate. Still, the complex controls on sediment transport, more specifically the transitions between detachment, transport, and supply limited streams are not well defined in natural systems. Continued long-term studies of tracer gravel will provide additional insight into this important geomorphic feature that is commonly used for stream restoration and remediation, providing public and private managers with additional data and potentially better designs for future projects.

3 Methods

3.1 Introduction

The study reach at Oak Creek was outfitted with a RFID antenna system capable of detecting individually tagged tracer particles as they were transported downstream with exact times and dates. The array system consists of a main reader box that is connected to three separate fixed antennas stretched across the stream channel within 150 meters of each other (Figure 3.1), where the most downstream antenna is ~20m upstream of the weir that was previously used to collect the data on bedload transport (Milhous, 1973). Transport events for gravel occurred during the winter months of each year but some years the peak flow was not enough to move tracers. In addition to fixed antennas tracking particle movement, a mobile reader box and handheld antenna was utilized to record tracer positions at the end of the winter months after all potential tracer movement had finished. Close to 3,000 tracer particles were deployed between 2016-2020, beginning near the most downstream antenna and stretching 600 meters upstream to a culvert. The goal of tracer deployment numbers and positions were to maintain a constant concentration of tracers throughout the study reach and antenna array.

To calculate bedload transport rates, the several deployments of gravel were configured to resemble a steady tracer injection, without the need to wait for all tracers to pass the antenna array, a potentially infeasible task. With the objective of keeping a steady concentration of tracers on the bed, both the count rate and optimal tracer concentration raise potential difficulties when developing transport rates. The count rate was defined as the number of tracers in motion

at an antenna at a particular point in time and is equivalent to the inverse of the mean inter-arrival time. An inter-arrival time is defined a pair of arrivals of different tracers at the same plane, so the upstream or downstream detection range of an antenna. Each antenna can only detect a single tracer at a time, so if tracer concentration on the bed is too large, data will potentially be lost. If tracer concentration on the bed is too low, recording small enough interarrival times during instances of uniform steady flow may not be achievable. Immobile tracers near an antenna also inhibit an antenna's ability to detect tracers that move in and out of its detectable range. Other than immobile tracers blocking detections, many other factors can influence the ability of a tracer to be detected, including differences in PIT tag sizes, particle orientation when passing antennas, strength of field parallel to antennas, and particle travel distances that exceed the ability to mobile track. Due to these factors, a simple efficiency of the RFID system can be evaluated based on the recovery rate of tracers using a combination of antenna array and mobile tracking detection records versus the total number of tracers that could be detected.

3.2 Design of System

3.2.1 Tagged Tracers

Gravel pieces were collected from Oak Creek, downstream of the study area, and embedded with PIT tags, each with a unique radio-frequency identification (RFID) number. Using many drill bits, marine epoxy, and two PIT tag sizes, 12 mm x 2.12 mm and 23 mm x 3.65 mm, close to 3,000 tagged gravel pieces were deployed to the bed of Oak Creek, in eleven separate

deployments, and comprised four different sizes ranges, 11–16 mm; 16–32 mm; 32–64 mm; and 64–101.5 mm. Deployments were grouped together by their specific deployment date and grain size class. Tracer deployment distance ranged between 130 meters to 600 meters, where the most downstream tracers were positioned just upstream of the last antenna in the array system and as far upstream as a culvert, positioned over 600m from the previously mentioned weir. Detailed data about each specific deployment is shown in Table 3.1, including the number of tracers deployed, the grain size range, the distance tracers were deployed over, PIT tag size, and the date for which tracers were deployed.

3.2.2 Fixed Antennas Array

An array of three fixed antennas, placed flat on the streambed across the channel (Schneider et al., 2010), were used to monitor tracer movement. The antennas were constructed from single loops of heavy-gauge wire and were held within PVC pipes. The shape of each antenna was configured as a long, thin rectangle, where the long sides span the channel width. The long and short sides are held together with right-angle “elbows” at the ends. Antennas were secured in place by several cord to steel soil anchors embedded in both the stream banks and bed.

The three antennas were attached, via shielded coaxial cables, to an assemblage of circuit boards comprised of a reader/controller, a radio-frequency module, a data-logger, and a four-way multiplexor, housed within a small weatherproof case. The system is powered by a single Tesla Model S™ 24-volt battery, which could continuously power the system for ~1 week. Before utilization of the Tesla battery, lead acid batteries were used but could only continuously run the

system for ~2-3 days before needing to be switched out. Since the system did not need to be active during most of the year, the Marys River gauge and forecast was utilized to determine when transport at Oak Creek would likely occur. When flow on Mary's River were projected to rise to 2,000 CMS, the array system would be turned on to catch any potential tracer movements. Each antenna can record the proximity of one tracer per broadcast-receive period, which broadcast between 123.2. kHz and 134.2 kHz. The time between the end of the broadcast-receive period and the beginning of the next must at least be long enough for the other multiplexed antennas to take their turns, but additional waiting time can be added to conserve power. The operating voltage range of the instrument assemblies is 7-24V and the controller are programmed to shut down when battery voltage drops below 10 V, and the fully charged battery may supply 14 V.

3.2.3 Mobile Tracking Antenna

To record tracer positions between antennas and outside of the array, another reader box and circuit board assemblage, powered by lead acid batteries, were carried by backpack, and powers a small, handheld antenna. This process has been dubbed "mobile tracking" and is utilized to precisely locate tracers by moving the antenna over the entire length and width of the bed and gravel bars. The entire tracer deployment reach and the stream reach for hundreds of meters downstream of the last antenna were monitored with the handheld antenna to locate as many tracer positions as possible. Distances were recorded using a hip-chain with several known tie-off positions along the study reach. An external plug for the antenna and an external switch for the instrument assembly allows power-up and shut down by a single operator without removing

the backpack. Mobile tracking occurred at the end of each water year so tracer positions could be compared with positions recorder from previous years to determine if a tracer had moved along the bed surface or was immobile.

3.3 Calculation of Transport Rate

Using a mass balance approach (Hudson and Fraser, 2005), the expression for calculating unit transport rate from the detection of passing tracers with a uniform concentration on the bed

(Equation 1)
$$q_i = \frac{\dot{n}_i V_{pi}}{B} \frac{F_i}{f_{Ti}},$$

where, for the *i*th size class, $\dot{n}_i$ is count rate, i.e., the number of tracers passing an antenna per time [T^{-1}]; V_{pi} is volume of a single particle [L^3]; B is channel width [L]; F_i is the fraction of bed surface covered by the grain size; and f_{Ti} is the tracer concentration, i.e., the fraction of the bed surface covered by tracers; and a uniform tracer concentration requires uniform placement not only in the vicinity of the detector, or throughout the antenna array, but also upstream for a distance great enough so the tracer concentration at the points of detection does not diminish.

Count events used to measure $\dot{n}_i$ are analogous to particles breaking a plane, and in this case, tracers either entering or leaving the readable range of an antenna. As long as tracer do not fall out of the detectable range of an antenna, each antenna will record particles breaking two planes, one upstream of the antenna and the other downstream of the antenna. For each passing tracer, arrival at the upstream plane is recorded by the earliest detection, and arrival at the downstream

plane is recorded by the latest detection. If the passage of a particle in the *i*th size class through either plane is a Poisson process with inter-arrival times described by a random variable, then it is justifiable to assume that the two random variables describing inter-arrival times at the two planes are independent and identically distributed as long as the controlling variables are equivalent. In simple terms, any two successive arrivals of different particles at the sample plane defines a sample inter-arrival time, but the time between arrival of a single particle at the upstream and downstream plane does not represent a sample inter-arrival time.

According to this probabilistic model, the count rate, $\dot{n}_i$, is a random variable that is determined by characterizing the distribution of inter-arrival times. For a count rate to be applicable for use with (equation 1), estimation of the expected value, or mean, of the random variable, is implied, and the count rate is equivalent to the inverse of the mean inter-arrivals time,

(Equation 2) $$\dot{n}_i = 1/\overline{T_{ai}}$$

Where T_{ai} is the random variable representing inter-arrival time, and $\overline{T_{ai}}$ is its mean, or technically, the sample mean, which is an estimation the mean of the underlying distribution. Since inter-arrival times are dependent on a variable that changes in time, it must be small enough relative to the time during which the random variable is stationary. For the Poisson process to function, the underlying distribution of the mean count rate needs to be exponentially distributed, so mean interarrival times must be equal to the standard deviation of those times. Using this theoretical model, interarrival times that were too large could be removed from the dataset as outlier detections.

3.4 Tracer Concentration

Areal concentration of tagged particles on the bed, f_{Ti}, was determined using a bed averaged tracer particle decay function based on characteristic from each individual deployment. First, a total study area is determined from the length of bed which tracers are deployed over and an average stream width for the reach. The area of coverage of tracers on the bed could then be calculated from the numbers of tracers present on the surface of the bed. After the deployment of tracers to the surface of the bed at Oak Creek, particles were assumed to be on the surface and available for transport once discharge increased. From the total study area and the area of coverage of tracers on the bed, the percent of tracer coverage per bed area could be determined. Lastly, the percent of tracer coverage per bed area is compared with the predicted sum of integrated transport from each water year (Figure 3.2-3.10). Tracer concentration for each deployment were calculated from the fitted exponential functions, where the "x" value in the exponent was determined from the sum of the integrated transport from the time of tracer deployment. The integrated transport was calculated from the predicted transport from the Parker (1990) model and summed for the entire period after a tracer was deployed. Table 3.2-3.4 detail minimum and maximum values for previously mentioned characteristics used to evaluate tracer concentrations.

Since mobile tracking occurred at the end of each water year, each characteristic for evaluating tracer concentration on the surface of the bed needed to be reevaluated. The most important aspect of year-to-year reevaluation were determining the number of tracers that have moved

passed the last antenna in the array and the number of immobile tracers. Tracers that moved out of the antenna array could be found from a combination of both final detections at antenna 3 and mobile tracking detections downstream of antenna 3. If a tracer moved out of the array without getting detected by antenna 3, mobile tracking would likely pick it up somewhere downstream of that antenna. The number of immobile tracers was determined by evaluating mobile tracking records and finding tracers that did not move a substantial distance from the previous year. From year-to-year mobile tracking records of transport distances, an error associated with hip-chain measurements could be determined and support the identification of immobile tracers from ones that moved. Figure 3.11 illustrates total tracers transport distance for water year 2017 for deployment 1 to help distinguish mobile from immobile tracers. The hip-chain mobile tracking method with several tie-off positions was utilized to minimize error associated with different tracking events and negative transport values helped to place limits between tracers that were immobile or on the surface. Negative transport distances are present because exact repeats of monitoring the stream while hovering the mobile antenna over all areas is an impossible task, even with several known tie-off positions. To account for this error, transport distances near +/-10 meters was used to distinguish immobile tracers from tracers that likely moved. The +/-10 meter distance was chosen due to the break in slope of the transport distances and where tracer distances began to avoid being cluster together, assuming the clustering points indicated immobile tracers. Known tracer positions upstream of the last antenna for deployment 1C are shown in Figure 3.12.

For each deployment of tracers, a substantial number of tracers can go undetected from year-to-year, and many tracers are never detected by the antenna array or from mobile tracking. Due to

these additional errors, a minimum and maximum number of tracers on the surface can be reconciled. The minimum values are based on the number of tracers that are detected, while the maximum values are determined by adding all unknown tracer positions to the minimum value. Though the efficiency of the system does not affect data quality, it does mean the loss of substantial data and potential inter-arrival times that could yield more transport rates. Since a minimum and maximum number of tracers on the surface of the bed could be determined, two decay functions were estimated for each deployment, acting similarly as error bars for transport rates.

3.5 Oak Creek Hydrograph

As previously mentioned, the Marys River future forecasts can be used to estimate when to turn on the antenna array system so detections of tracers passing antennas could be gathered without having to constantly have the system running. For substantial time periods during this study, continuous discharge data was not available, so a relation of discharge events between the Mary's River and Oak Creek was determined for predicting integrated transport between times where discharge data was available. Predicted sum of integrated transport is essential for characterizing tracer concentrations on the bed from year-to-year. Using a stage-discharge relationship from known pressure logger data in the study reach at Oak Creek (Figure 3.13), and modeled discharge peaks were compared with peaks on Mary's River (Figure 3.14). For four known periods of tracer movement during the 2017 water year, the sum of integrated transport was determined to be 0.76 m^2 and from the Marys River-Oak Creek relation, the sum of integrated transport was estimated to be 0.79 m^2. For three known periods of tracer movement

during the 2021 water year, the sum of integrated transport was determined to be 0.56 m^2 and from the Marys River-Oak Creek relation, the sum of integrated transport was estimated to be 0.58 m^2. Though R^2 values were low for the comparison, integrated transport for known periods were similar to that when using the estimated comparison and was concluded to be a reliable estimator for times when discharge data was unavailable.

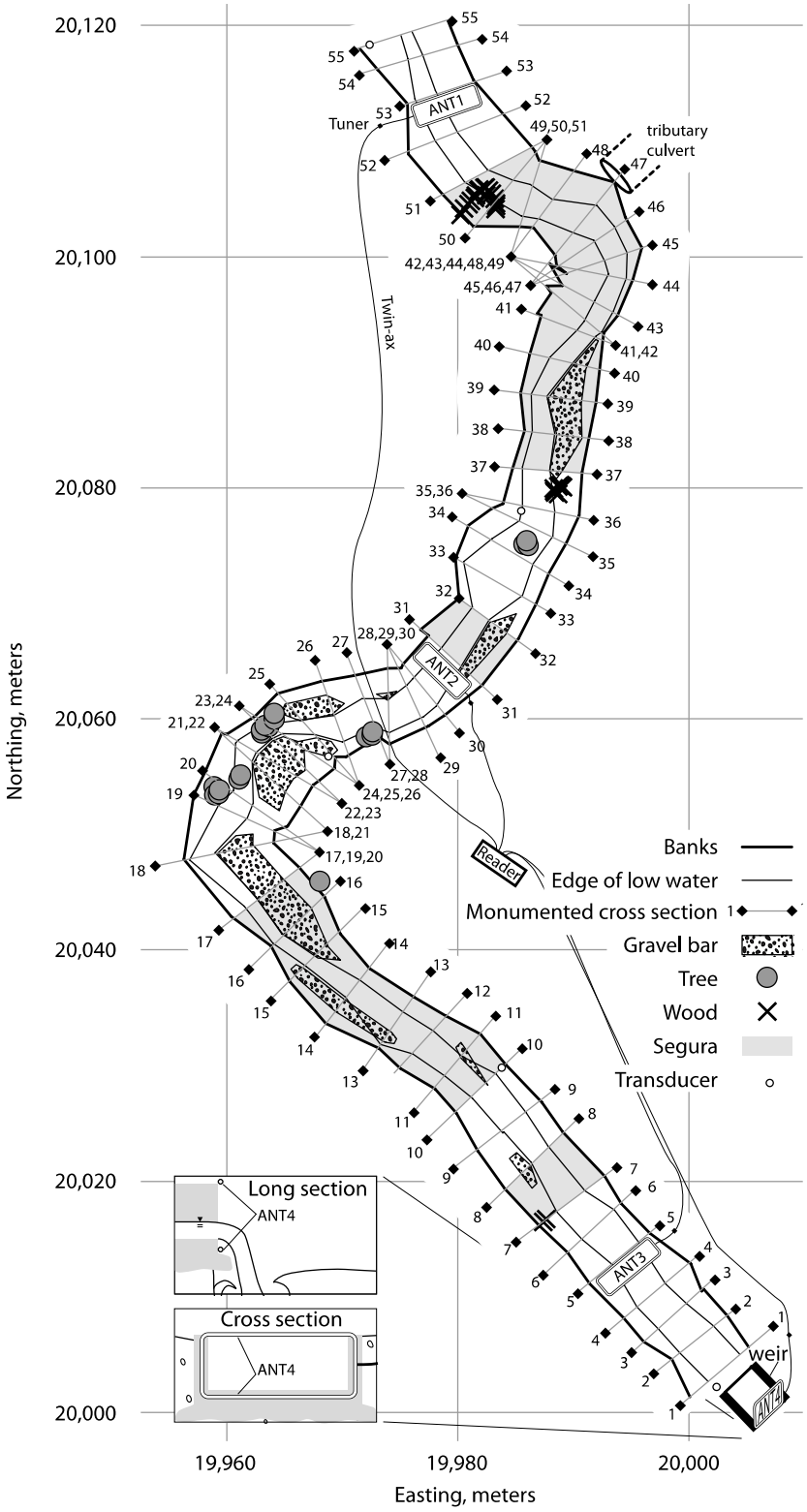

Figure 3.1. Map of antenna positions and additional in-stream features through antenna array. The antenna 4 location is at the downstream limit of the weir and was not used in this study. Data and map are from a combination of work by Stephen T. Lancaster, Jon Sanfilippo, Catalina Segura, and Scott Katz.

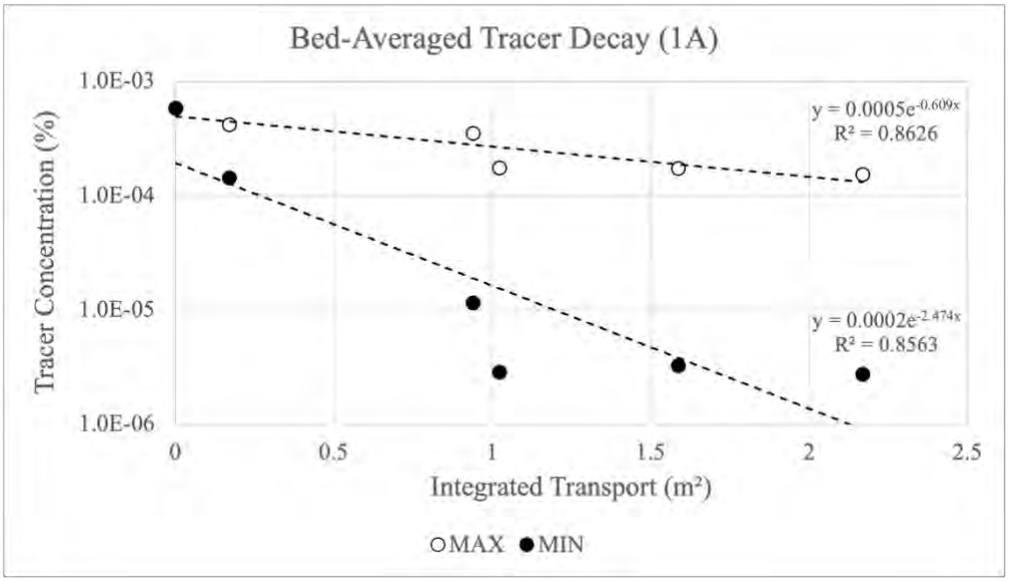

Figure 3.2. Bed-averaged tracer decay plot for Deployment 1A and exponential function fits for both minimum and maximum numbers of tracers on the surface.

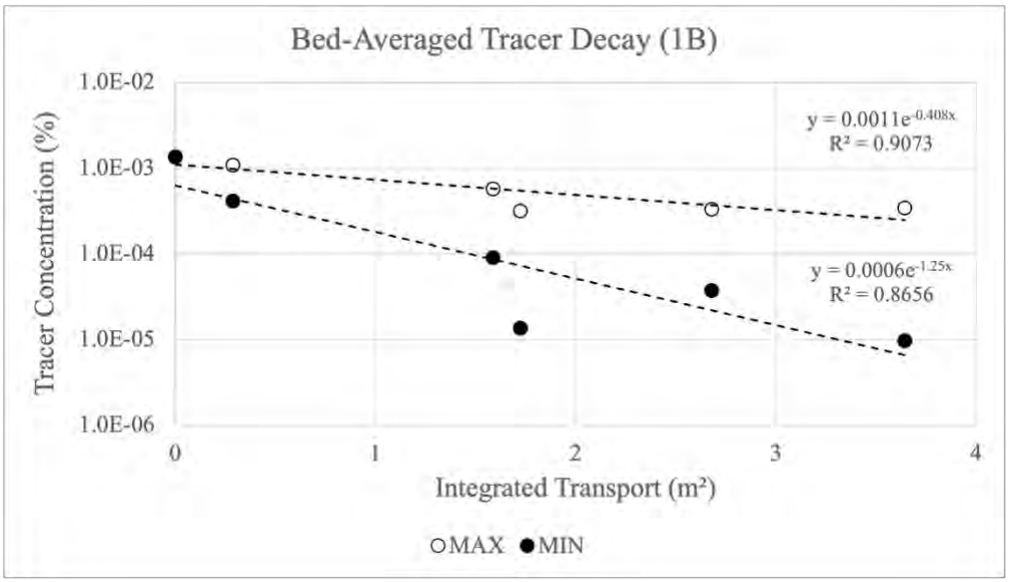

Figure 3.3. Bed-averaged tracer decay plot for Deployment 1B and exponential function fits for both minimum and maximum numbers of tracers on the surface.

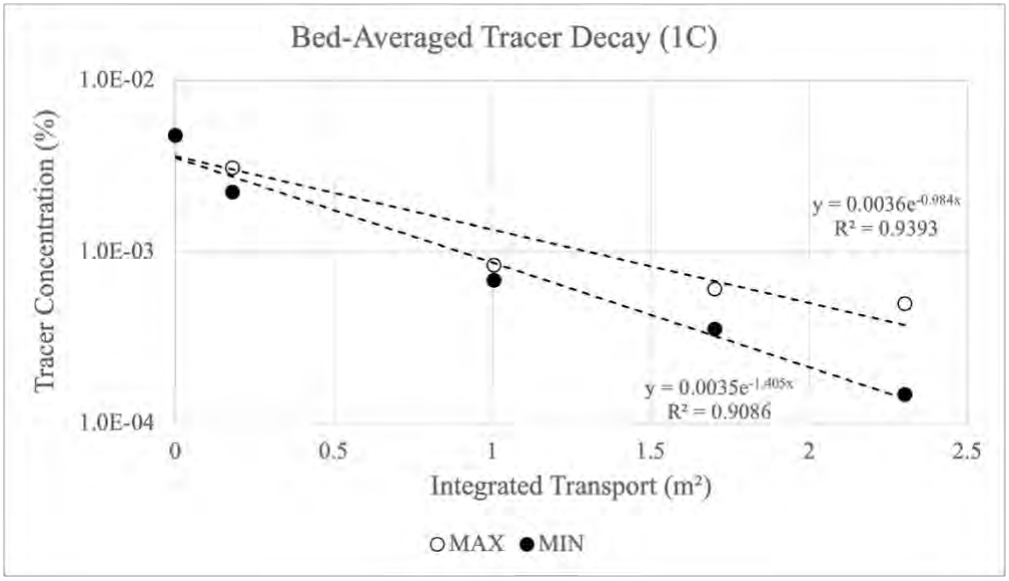

Figure 3.4. Bed-averaged tracer decay plot for Deployment 1C and exponential function fits for both minimum and maximum numbers of tracers on the surface.

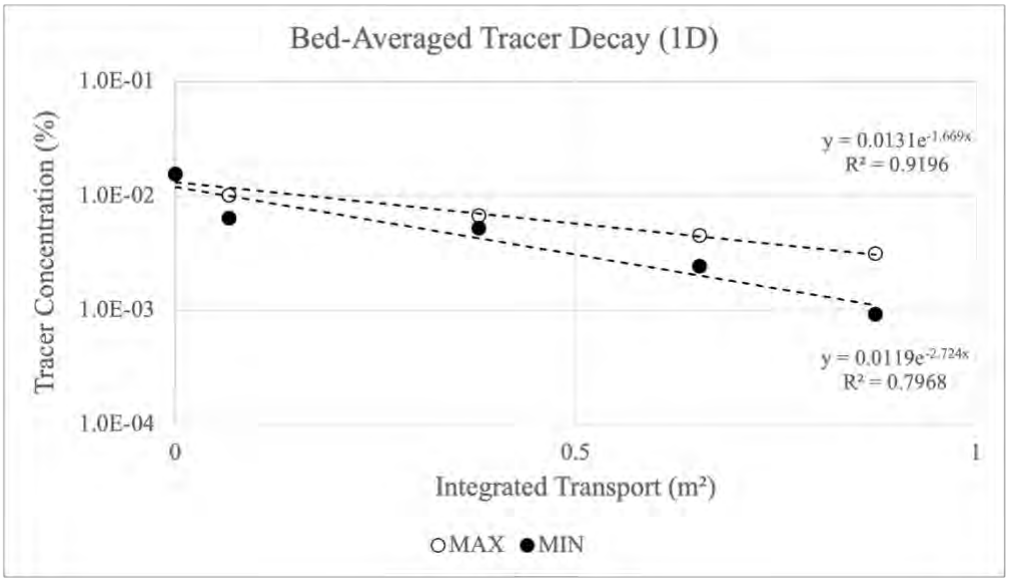

Figure 3.5. Bed-averaged tracer decay plot for Deployment 1D and exponential function fits for both minimum and maximum numbers of tracers on the surface.

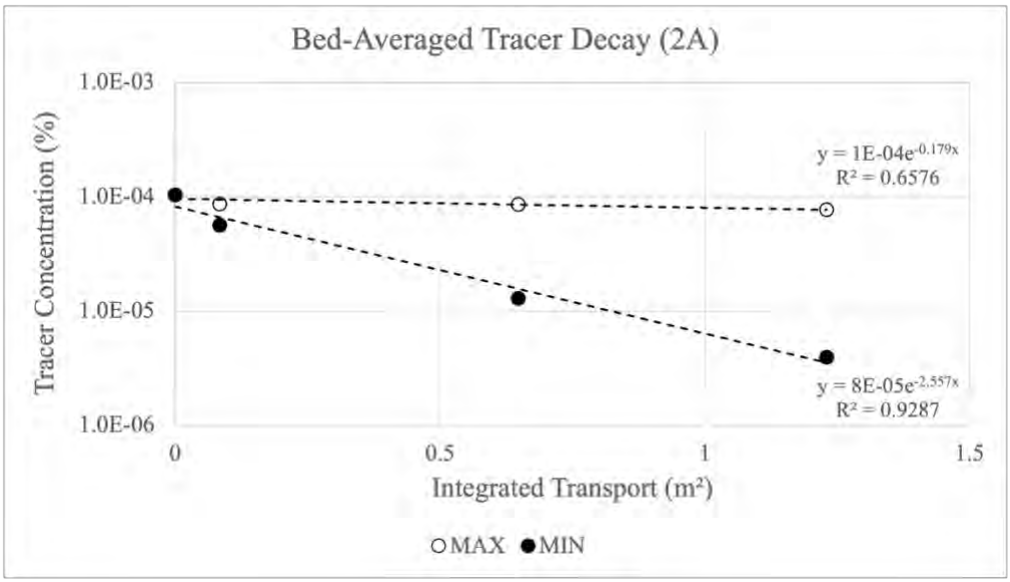

Figure 3.6. Bed-averaged tracer decay plot for Deployment 2A and exponential function fits for both minimum and maximum numbers of tracers on the surface.

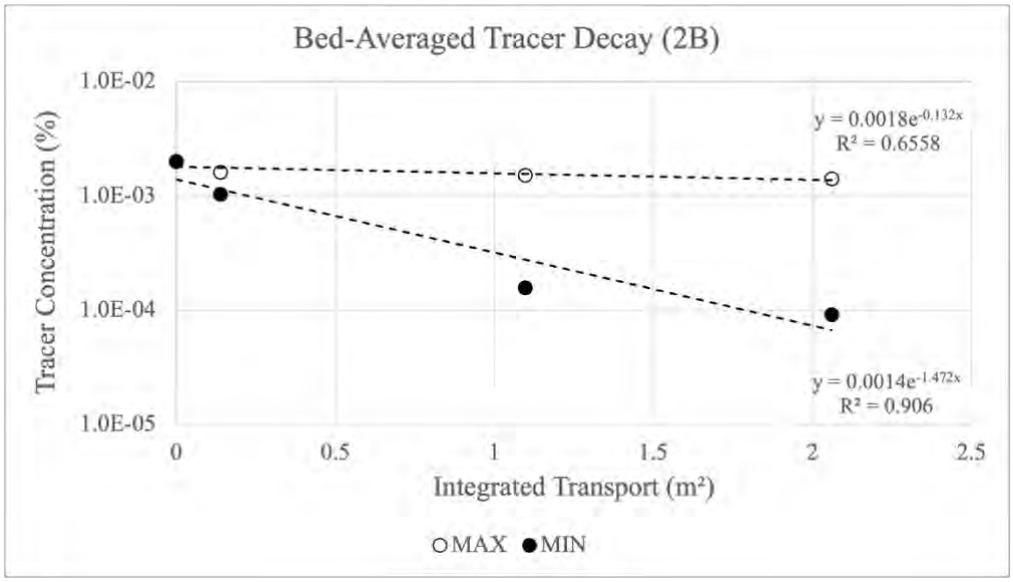

Figure 3.7. Bed-averaged tracer decay plot for Deployment 2B and exponential function fits for both minimum and maximum numbers of tracers on the surface.

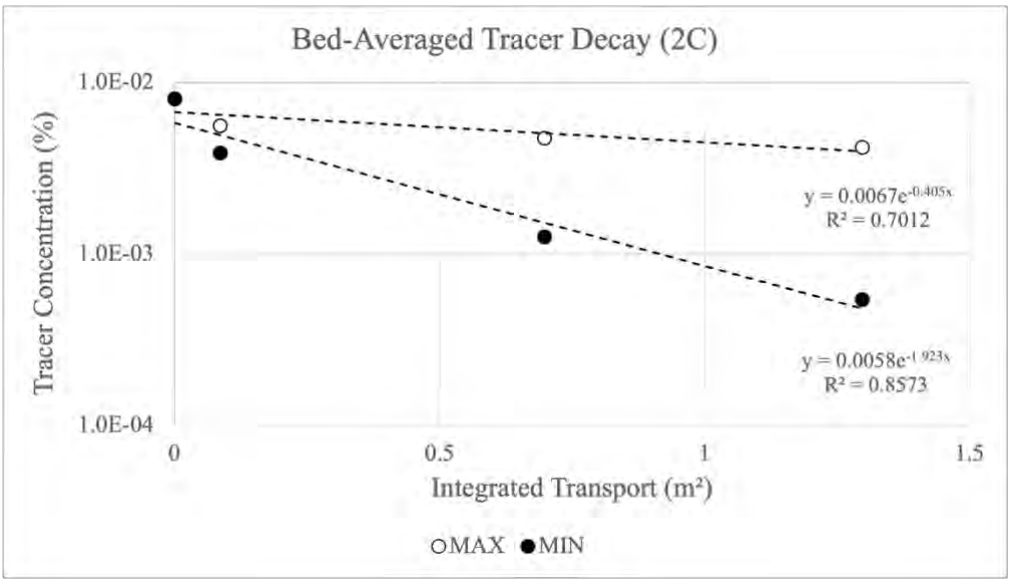

Figure 3.8. Bed-averaged tracer decay plot for Deployment 2C and exponential function fits for both minimum and maximum numbers of tracers on the surface.

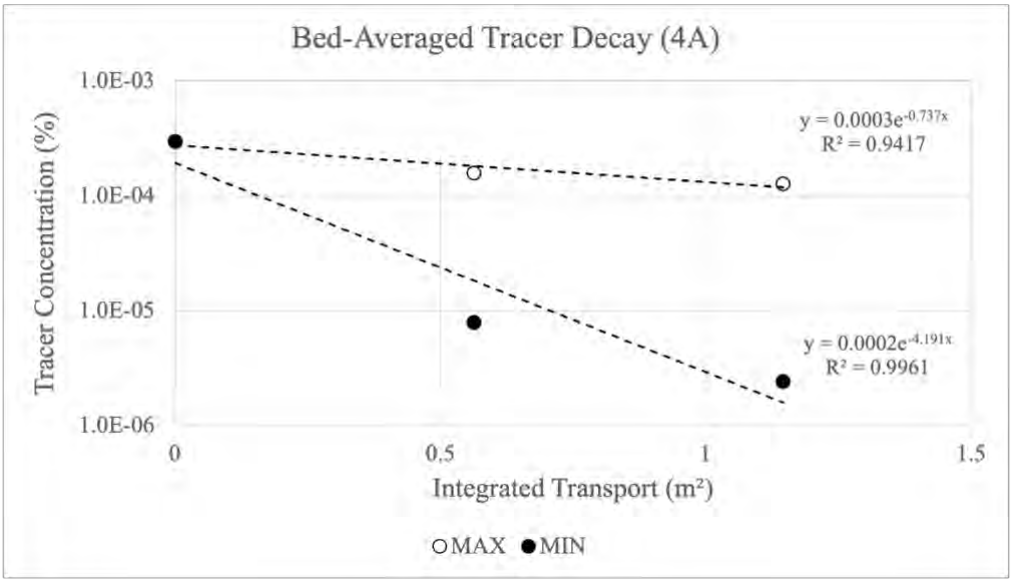

Figure 3.9. Bed-averaged tracer decay plot for Deployment 4A and exponential function fits for both minimum and maximum numbers of tracers on the surface.

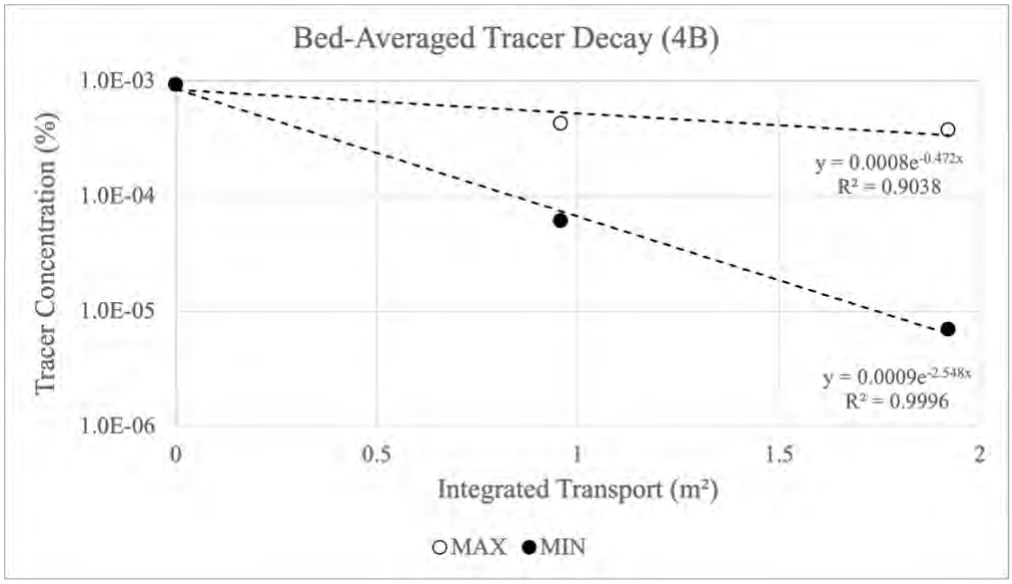

Figure 3.10. Bed-averaged tracer decay plot for Deployment 4B and exponential function fits for both minimum and maximum numbers of tracers on the surface.

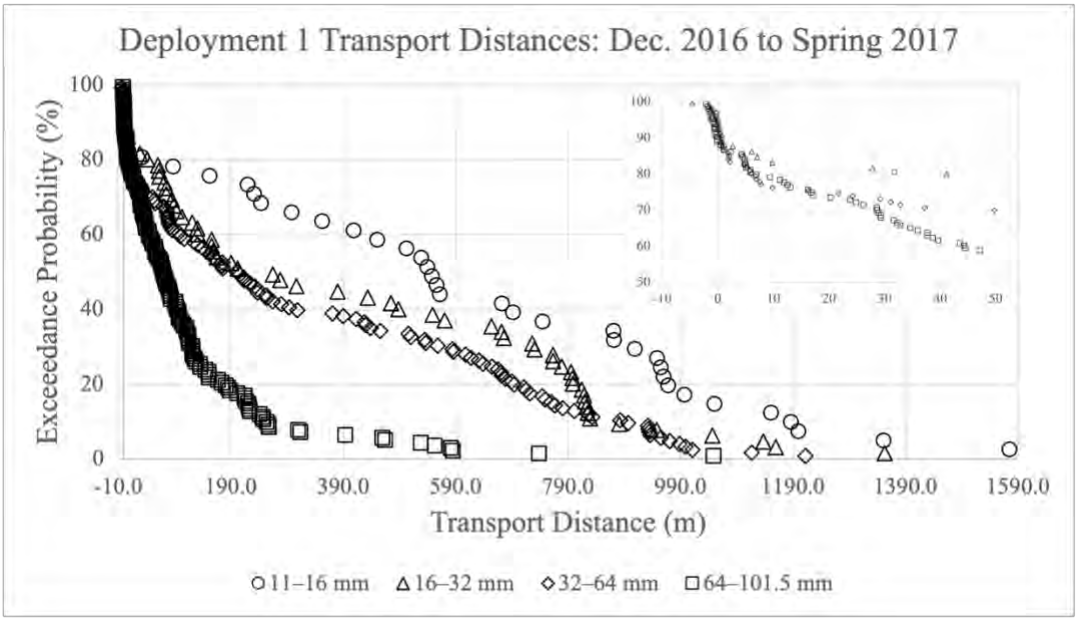

Figure 3.11. Cumulative transport distances between December 2016 and Spring 2017 for each grain size class from deployment 1. Inset figure is a subset of the data up to 50 meters in transport distance to show where a break in slope is present between five and ten meters that identifies where to distinguish between mobile and immobile tracers. Negative distances are associated with general error in mobile tracking technique.

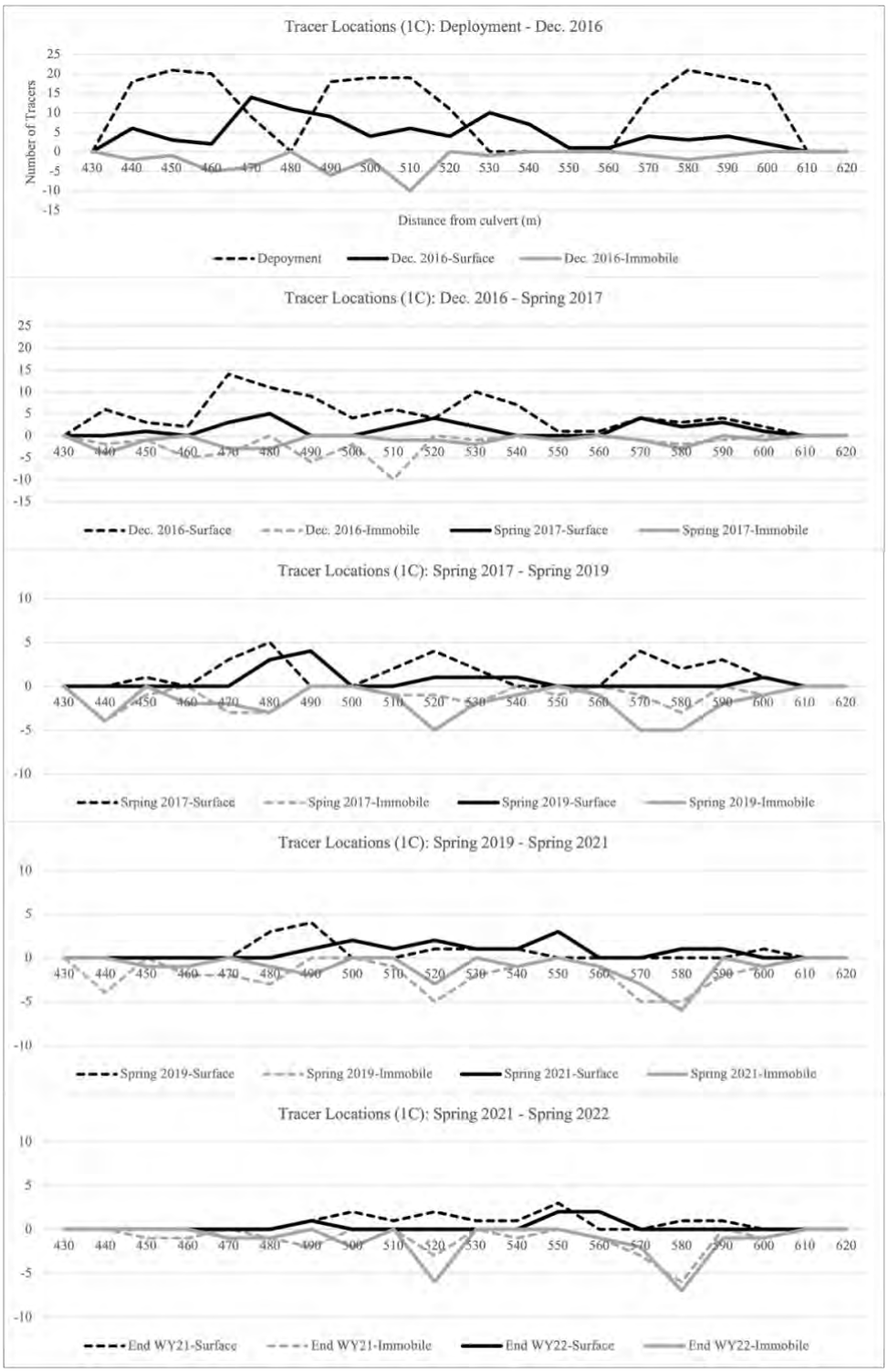

Figure 3.12. Tracer locations upstream of the last antenna position, antennas are located at 477 m, 529 m, and 611 m. Values along the x-axis are distances downstream of a culvert used as a known benchmark position. Y-axis values are numbers of tracers at each distance, positive values are tracers on the surface and negative values are immobile tracers.

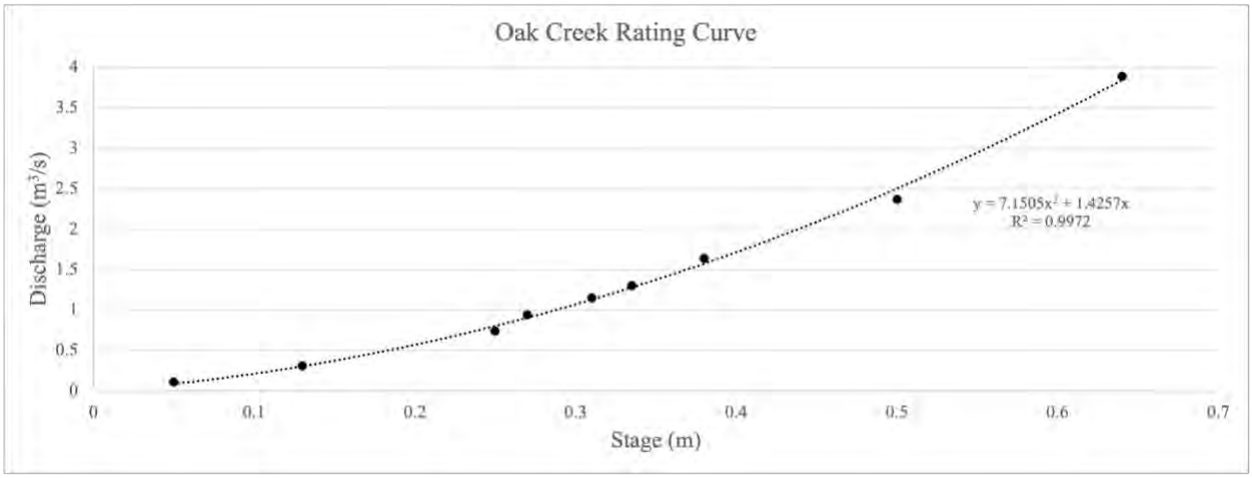

Figure 3.13. Stage-discharge relationship for study reach at Oak Creek from a combination of data gather for this study and from Katz et al. (2018).

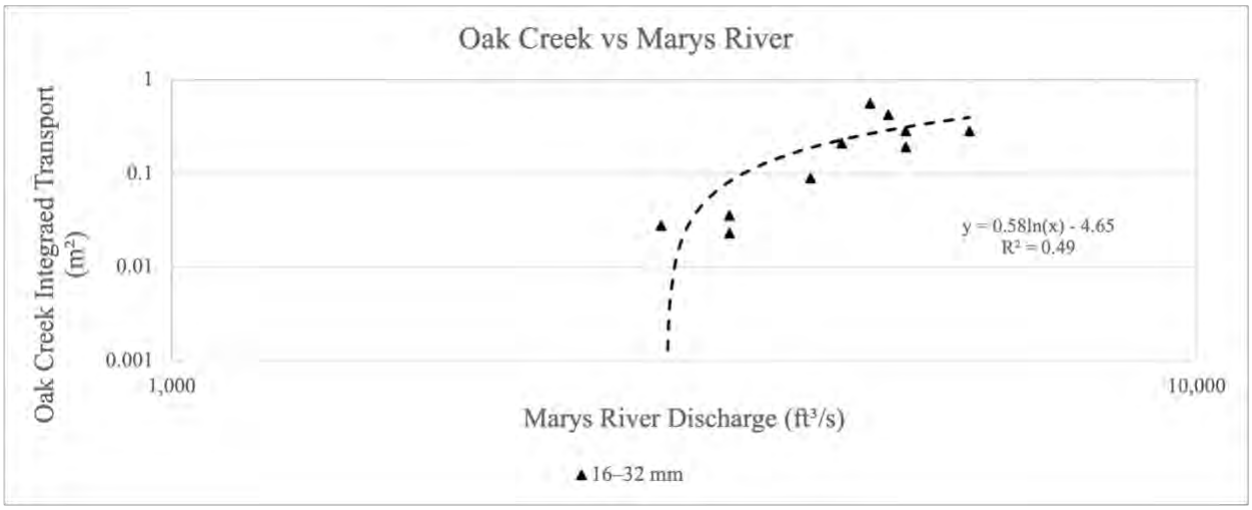

Figure 3.14. Comparison between peak discharge events on Marys River and integrated transport on Oak Creek during known events where substantial tracer movement occurred, each axis is log scaled. Equation and R^2 values in graph are listen in order, from top to bottom, from smaller to large grain size classes. A log fit to the data points produced the highest R^2 values for the relationship.

Table 3.1. Records related with each tracer deployment.

Deployment 1	**1A**	**1B**	**1C**	**1D**
Number of tracers	249	241	206	208
Grain size (mm)	11-16	16-32	32-64	64-101.5
Distance deployed over (m)	134	176	171	159
PIT tag size (mm)	12 x 2.12	12 x 2.12	23 x 3.65	23 x 3.65
Deployment date	10/30/2016	10/30/2016	10/30/2016	10/30/2016
Deployment 2	**2A**	**2B**	**2C**	
Number of tracers	196	936	427	
Grain size (mm)	11-16	16-32	32-64	
Distance deployed over (m)	591	466	212	
PIT tag size (mm)	12 x 2.12	12 x 2.12	12 x 2.12	
Deployment date(s)	11/18/2018, 12/6/2018	11/18/2018, 12/6/2018	11/18/2018, 12/6/2018	
Deployment 3	**3A**	**3B**		
Number of tracers	22	22		
Grain size (mm)	11-16	16-32		
Distance deployed over (m)	75	75		
PIT tag size	12 x 2.12	12 x 2.12		
Deployment date	2/12/2019	2/12/2019		
Deployment 4	**4A**	**4B**		
Number of tracers	148	148		
Grain size range (mm)	11-16mm	16-32mm		
Distance deployed over (m)	156m	156m		
PIT tag size (mm)	12 x 2.12	12 x 2.12		
Deployment date	2/8/2020	2/8/2020		

Table 3.2. Statistics from each year for Deployment 1 used to determine tracer concentration.

Deployment 1A						
Mobile Tracking	Deployed	Dec. 2016	Spring 2017	Spring 2019	Spring 2021	Spring 2022
Tracers on surface	249	61-207	4-121	1-61	1-56	1-56
Distance along bed (m)	130	130-160	110	110	90-100	110
Study area (m^2)	490	490-570	400	400	350-370	420
Tracer coverage (m^2)	0.3	0.07-0.2	0.005-0.1	0.001-0.07	0.001-0.06	0.001-0.06
Tracer coverage on bed (%)	0.058	0.014-0.042	0.0012-0.035	0.00029-0.018	0.00033-0.017	0.00027-0.015
Integrated Transport (m^2)	0	0.2	0.9	1.0	1.6	2.2
Deployment 1B						
Mobile Tracking	Deployed	Dec. 2016	Spring 2017	Spring 2019	Spring 2021	Spring 2022
Tracers on surface	241	71-187	15-95	2-47	4-50	1-45
Distance along bed (m)	180	170	170	150	110-150	100-130
Study area (m^2)	640	620	600	530	390-550	370-480
Tracer coverage (m^2)	0.87	0.26-0.68	0.054-0.34	0.0072-0.17	0.014-0.18	0.0036-0.16
Tracer coverage on bed (%)	0.14	0.041-0.11	0.0090-0.057	0.0014-0.032	0.0037-0.033	0.00097-0.034
Integrated Transport (m^2)	0	0.3	1.6	1.7	2.7	3.6
Deployment 1C						
Mobile Tracking	Deployed	Dec. 2016	Spring 2017	Spring 2019	Spring 2021	Spring 2022
Tracers on surface	206	91-126	27-33	11-16	14-24	5-17
Distance along bed (m)	170	160	160	160	160	140
Study area (m^2)	630	600	580	580	580	490
Tracer coverage (m^2)	2.9	1.3-1.8	0.39-0.48	0.16-0.23	0.20-0.35	0.072-0.25
Tracer coverage on bed (%)	0.48	0.22-0.31	0.068-0.083	0.028-0.040	0.035-0.061	0.015-0.050
Integrated Transport (m^2)	0	0.18	1.0	1.1	1.7	2.3
Deployment 1D						
Mobile Tracking	Deployed	Dec-2016	End WY17	Spring 2019	Spring 2021	Spring 2022
Tracers on surface	208	81-129	66-85	18-30	29-54	10-34
Distance along bed (m)	160	150	150	150	140	130
Study area (m^2)	580	550	550	560	520	470
Tracer coverage (m^2)	8.9	3.5-5.6	2.8-3.7	0.77-1.3	1.2-2.3	0.43-1.5
Tracer coverage on bed (%)	1.5	0.63-1.0	0.52-0.67	0.14-0.23	0.24-0.45	0.091-0.31
Integrated Transport (m^2)	0	0.067	0.38	0.41	0.65	0.87

Table 3.3. Statistics from each year for Deployment 1 used to determine tracer concentration.

Deployment 2A				
Mobile Tracking	Deployed	Spring 2019	Spring 2021	Spring 2022
Tracers on surface	196	105-161	23-159	7-144
Distance along bed (m)	590	580	560-580	560-580
Study area (m^2)	2200	2100	2000-2100	2000-2100
Tracer coverage (m^2)	0.22	0.12-018	0.026-0.18	0.0080-0.17
Tracer coverage on bed (%)	0.010	0.0056-0.0086	0.0013-0.0085	0.00039-0.0077
Integrated Transport (m^2)	0	0.084	0.65	1.2
Deployment 2B				
Mobile Tracking	Deployed	Spring 2019	Spring 2021	Spring 2022
Tracers on surface	936	489-781	69-720	39-677
Distance along bed (m)	470	470-490	440-480	420-480
Study area (m^2)	1700	1700-1800	1600-1700	1500-1700
Tracer coverage (m^2)	3.39	1.8-2.8	0.25-2.6	0.14-2.5
Tracer coverage on bed (%)	0.20	0.10-0.16	0.016-0.15	0.0091-0.14
Integrated Transport (m^2)	0	0.14	1.1	2.0
Deployment 2C				
Mobile Tracking	Deployed	Spring 2019	Spring 2021	Spring 2022
Tracers on surface	427	232-347	95-369	41-315
Distance along bed (m)	210	240-250	300-310	300
Study area (m^2)	780	870-900	1100-1200	1100
Tracer coverage (m^2)	6.2	3.4-5.0	1.4-5.3	0.60-4.6
Tracer coverage on bed (%)	0.80	0.39-0.56	0.13-0.47	0.054-0.42
Integrated Transport (m^2)	0	0.086	0.70	1.3

Table 3.4. Statistics from each year for Deployment 4 used to determine tracer concentration.

Deployment 4A			
Mobile Tracking	Deployed	Spring 2021	Spring 2022
Tracers on surface	148	6-120	2-118
Distance along bed (m)	160	240	260-290
Study area (m^2)	570	870	950-1100
Tracer coverage (m^2)	0.17	0.0069-0.14	0.0022-0.14
Tracer coverage on bed (%)	0.030	0.00079-0.016	0.00024-0.013
Integrated Transport (m^2)	0	0.6	1.2
Deployment 4B			
Mobile Tracking	Deployed	Spring 2021	Spring 2022
Tracers on surface	148	17-119	2-108
Distance along bed (m)	160	270	280
Study area (m^2)	570	1000	1000
Tracer coverage (m^2)	0.54	0.061-0.43	0.0072-0.39
Tracer coverage on bed (%)	0.094	0.0061-0.043	0.0070-0.038
Integrated Transport (m^2)	0	0.96	1.9

4 Results

4.1 Bedload Transport Rates

A total of 685 inter-arrival samples were gathered between the fall of 2016 through the spring of 2022, resulting in 66 bin-averaged bedload transport rates. Bins consist of 10 samples and were grouped together by similar discharges. From tracer concentration evaluations, both a minimum and maximum number of tracers on the surface were estimated, since each deployment had tracers that were not detected by either the antenna array or mobile tracking, and this resulted in a minimum and maximum transport rate for all samples. Between the minimum and maximum transport rates, the former is presumably a more probable rate because undetected tracers likely moved through the system without being detected and, in turn, are not present on the surface. A minimum number of tracers on the bed resulted in a higher transport rate and a maximum number of tracers on the bed resulted in a lower transport rate. Figure 4.1 shows an example of the minimum and maximum transport rates for all inter-arrival samples, while Figure 4.2-4.9 display bin-averaged transport rates from the four different sizes classes that tracer deployments consisted of. Figure 4.2-4.9 also illustrate the expected transport rate from Parker (1990) and measurements gathered from the previous vortex sampler that was used to calibrate the Parker model (Milhouse, 1973). Additionally, the bankfull conditions for the study area at Oak Creek is shown (Katz et al. 2018; Milhouse 1973), though discharge at the weir during this study was recorded above bankfull, and the stage-discharge relationship estimates discharges well above bankfull. Further, output from the Parker model was flattened to estimate transport at bankfull conditions.

The shape of the Parker model tends to level off at higher discharges and tracer data shows a nearly flat trend of transport across all discharges. In general, all bedload transport rates calculated from this study undershoot the estimated model for particles on the surface of the bed, particularly the smaller size classes. The two smallest tracer classes, 11–16 mm and 16–32 mm, undershoot the estimated model at all discharges by an order of magnitude or greater. Due to more tracers evading detection, maximum and minimum transport rates for the smaller size classes varied by an order of magnitude or greater. Smaller particles were over twice as likely to make it through the antenna array system and mobile tracking without being detected. Transport rates from the larger two class sizes, 32–64 mm and 64–101.5 mm, followed the estimated model more closely than the smaller class sizes. Data from the larger particles resulted in bin-averaged transport rates less than an order of magnitude off the estimated model, more closely resembling the results gathered from the previous vortex sampler. In all, tracer gravel transport rates were similar along all discharges, indicating possible deviations from the estimated model and other data gathered from the reach. Of the four size classes, the 16–32 mm and 32–64 mm showed signs of higher transport rates with climbing discharge while transport for the other two classes was mainly flat.

4.2 Additional Analysis of Transport Rates

Bin-averaged bedload transport rates determined were nondimensionalized using the Einstein parameter, q_b^*, and compared to the Shield's stress, τ^*, for each size class (Figure 4.10-4.13). Shields stress during varying flows were calculated from the bed-averaged shear stress for the

reach determined by Monsalve et al. (2020). Once bankfull conditions were met, shear stress was assumed to be constant and no longer increasing with discharge estimates. In general, no trends could be gathered from these comparisons, but weak trends could be observed in the 16–32 mm and 32–64 mm tracer size classes. The large numbers of points clustered at higher Shields stress for each size class indicates that more inter-arrival times were generated during bankfull conditions.

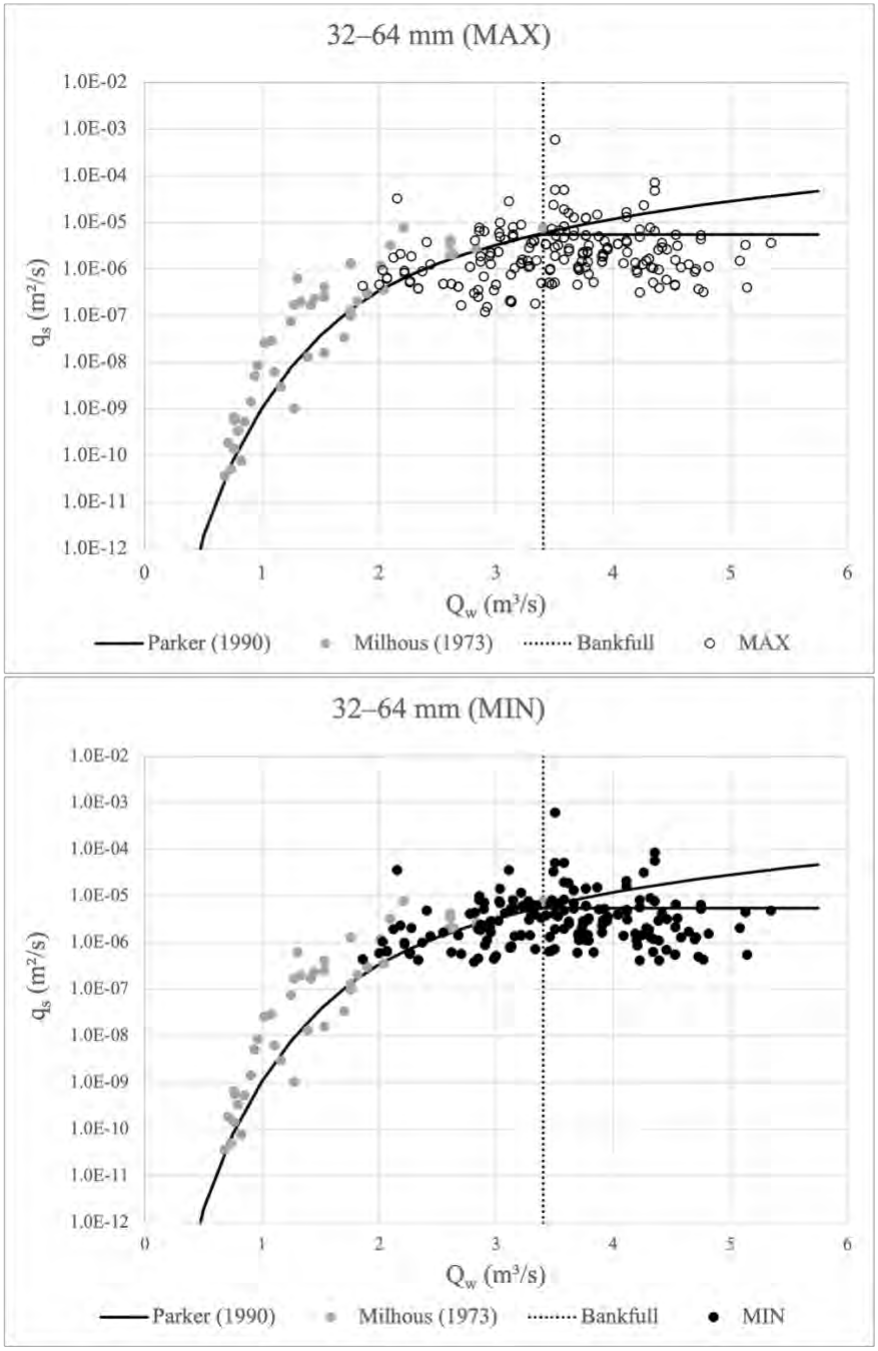

Figure 4.1. Cloud of individual sample points, from 32-64 mm size class, for maximum (top) and minimum (bottom) number of tracers on surface of the bed, resulting in minimum and maximum transport rate values. Transport rates are plotted against the related discharge for each sample. Solid black line is estimated transport rate for the grain size class based on the Parker (1990) model output and grey dots are data from vortex sampler (Milhous, 1973) used to calibrate the Parker model. The second, lower, Parker model output at higher discharges was leveled off to show bankfull conditions and the vertical, dotted line at 3.4 m^3/s displays the discharge at bankfull conditions. Y-axis is plotted in log scale.

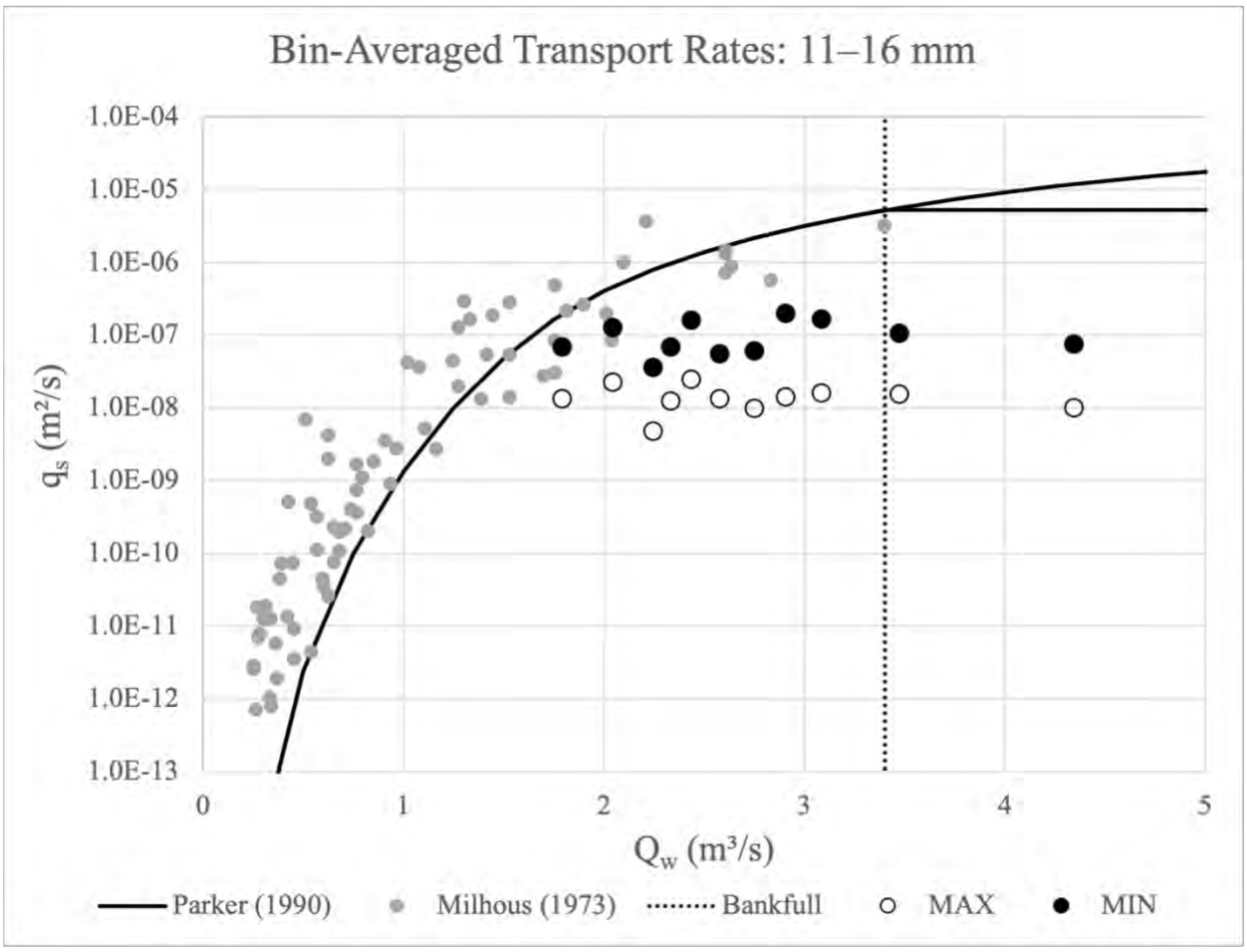

Figure 4.2. Bin averaged transport rates, from 16-32 mm size class, for estimated minimum (solid dots) and maximum (empty dots) transport rate values. Transport rates, q_s, are plotted against the related discharge, Q_w, for each bin and bins consists of ten samples. Solid black line is estimated transport rate for the grain size class based on the Parker (1990) model output and grey dots are data from vortex sampler (Milhous, 1973) used to calibrate the Parker model. The second, lower, Parker model output at higher discharges was leveled off to show bankfull conditions and the vertical, dotted line at 3.4 m^3/s displays the discharge at bankfull conditions. Y-axis is plotted in log scale.

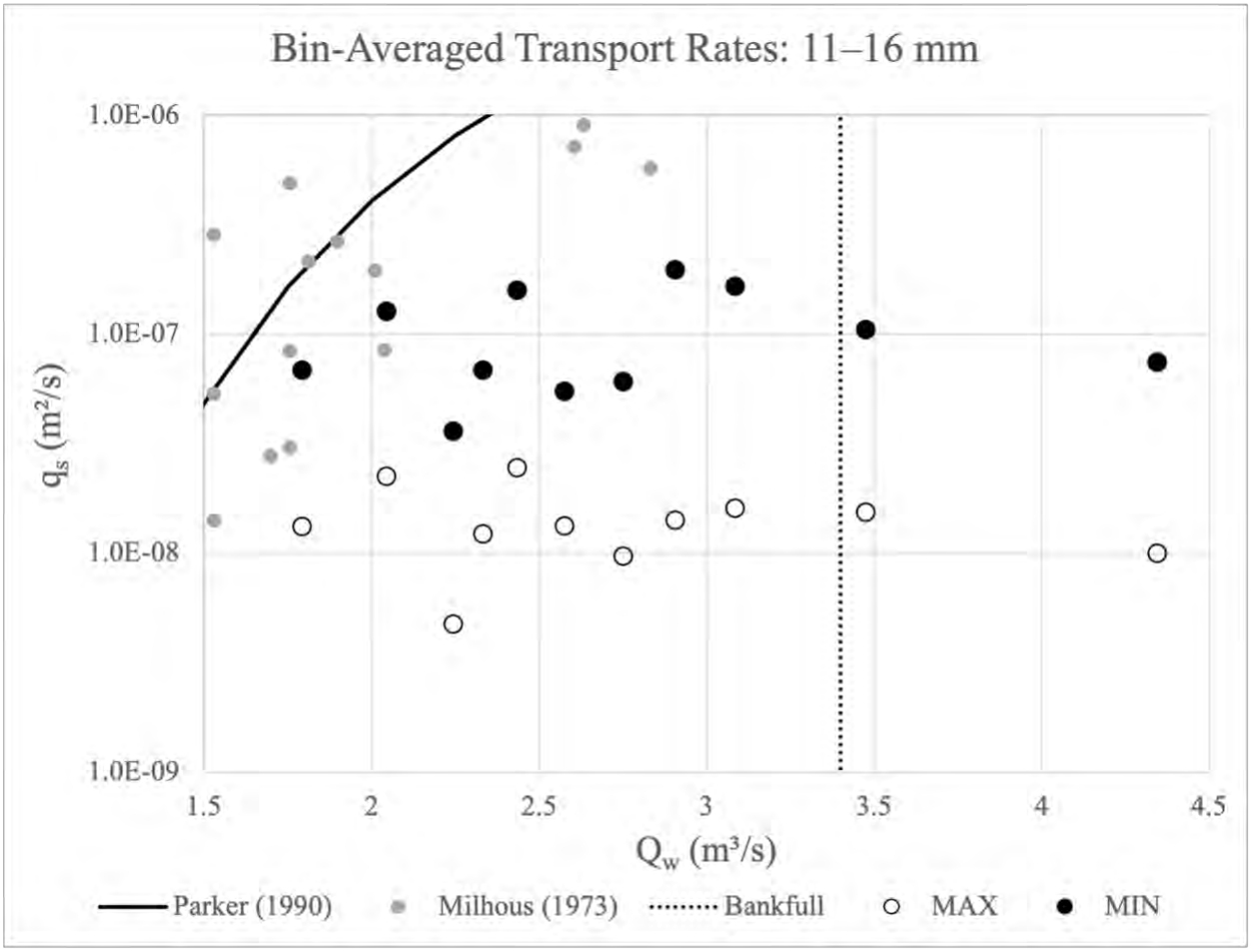

Figure 4.3. Same data and graph as Figure 4.2 but zoomed in on the bin-averaged transport rates from this study to show any trends between data points.

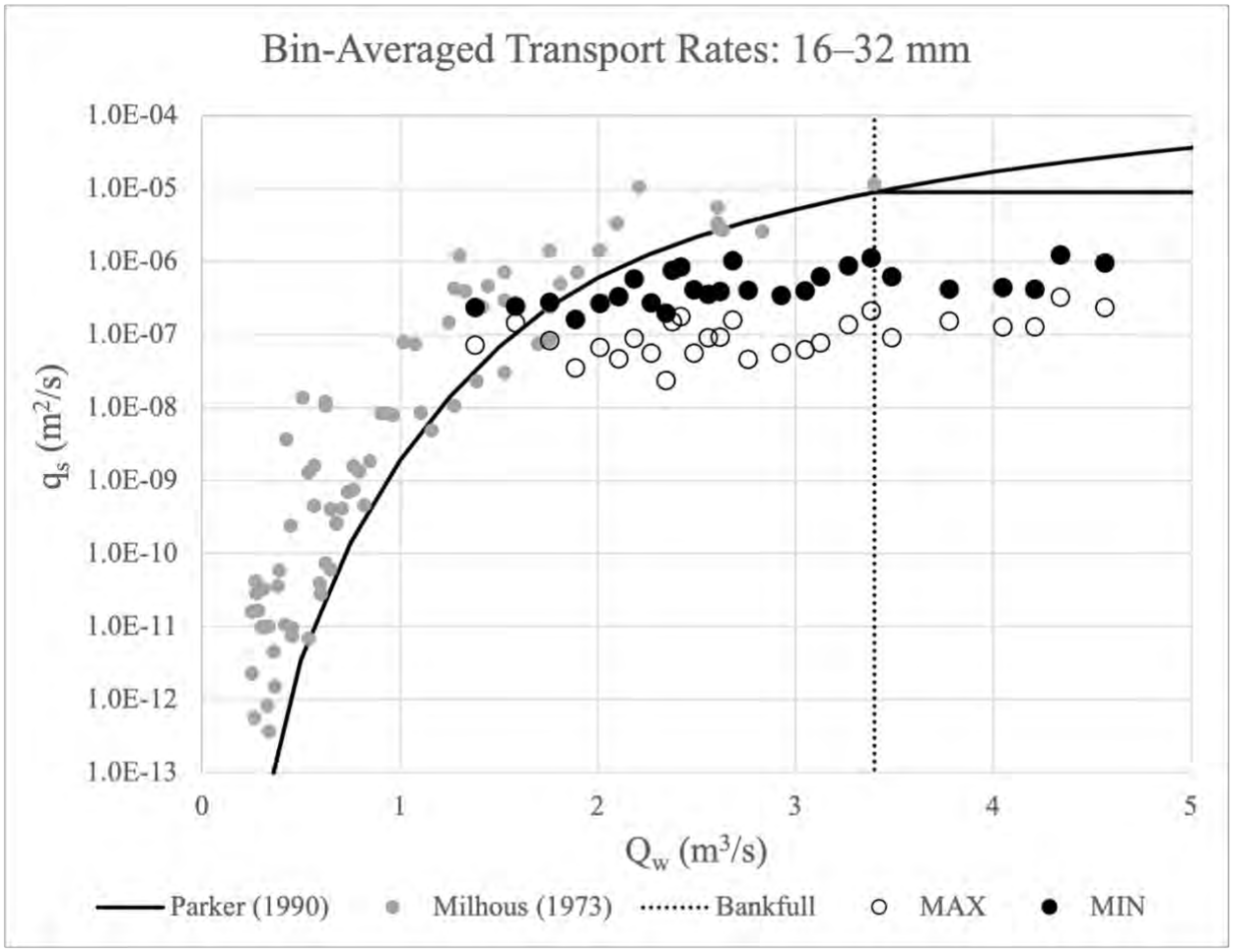

Figure 4.4. Bin averaged transport rates, from 16-32 mm size class, for estimated minimum (solid dots) and maximum (empty dots) transport rate values. Transport rates, q_s, are plotted against the related discharge, Q_w, for each bin and bins consists of ten samples. Solid black line is estimated transport rate for the grain size class based on the Parker (1990) model output and grey dots are data from vortex sampler (Milhous, 1973) used to calibrate the Parker model. The second, lower, Parker model output at higher discharges was leveled off to show bankfull conditions and the vertical, dotted line at 3.4 m^3/s displays the discharge at bankfull conditions. Y-axis is plotted in log scale.

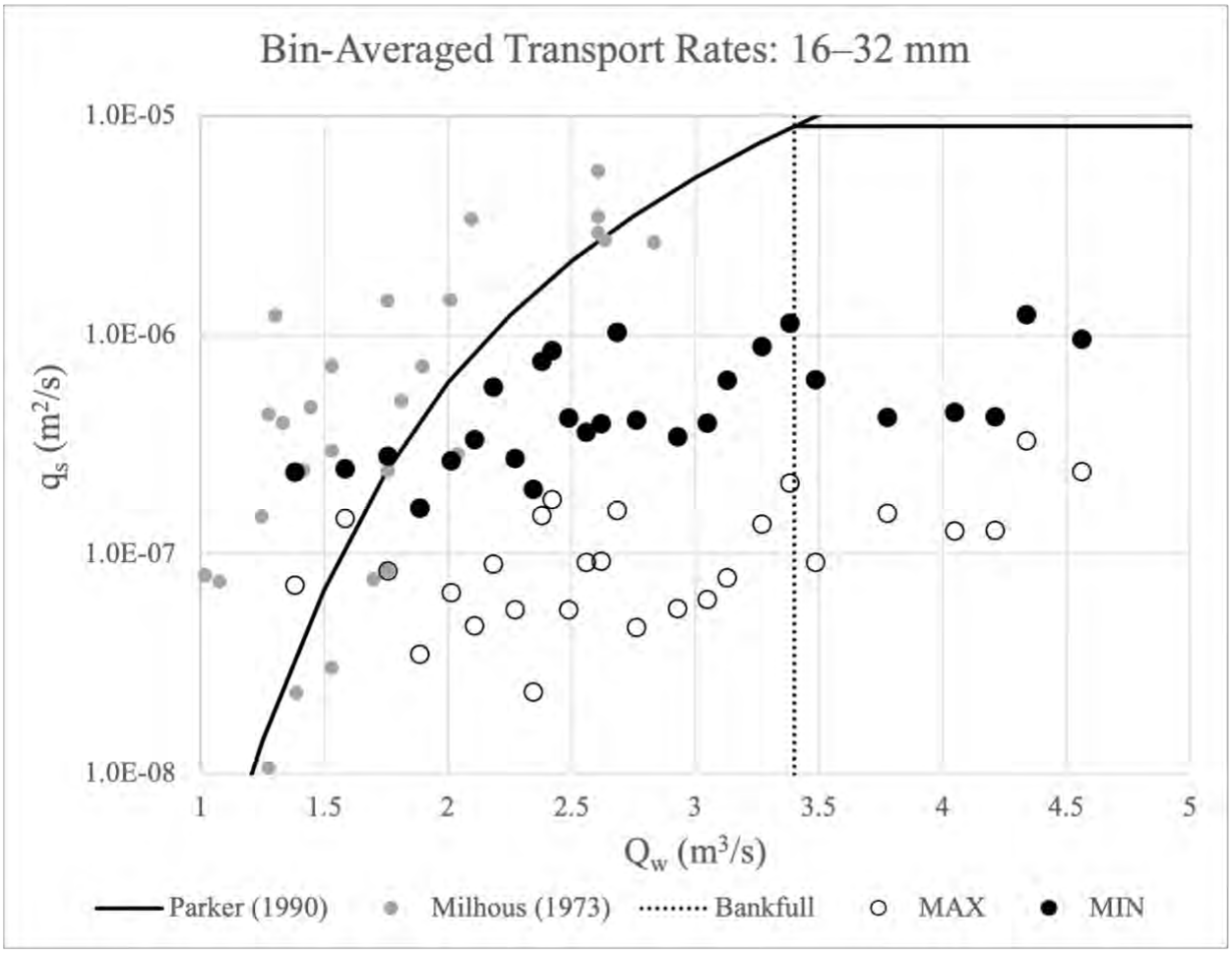

Figure 4.5. Same data and graph as Figure 4.4 but zoomed in on the bin-averaged transport rates from this study to show any trends between data points.

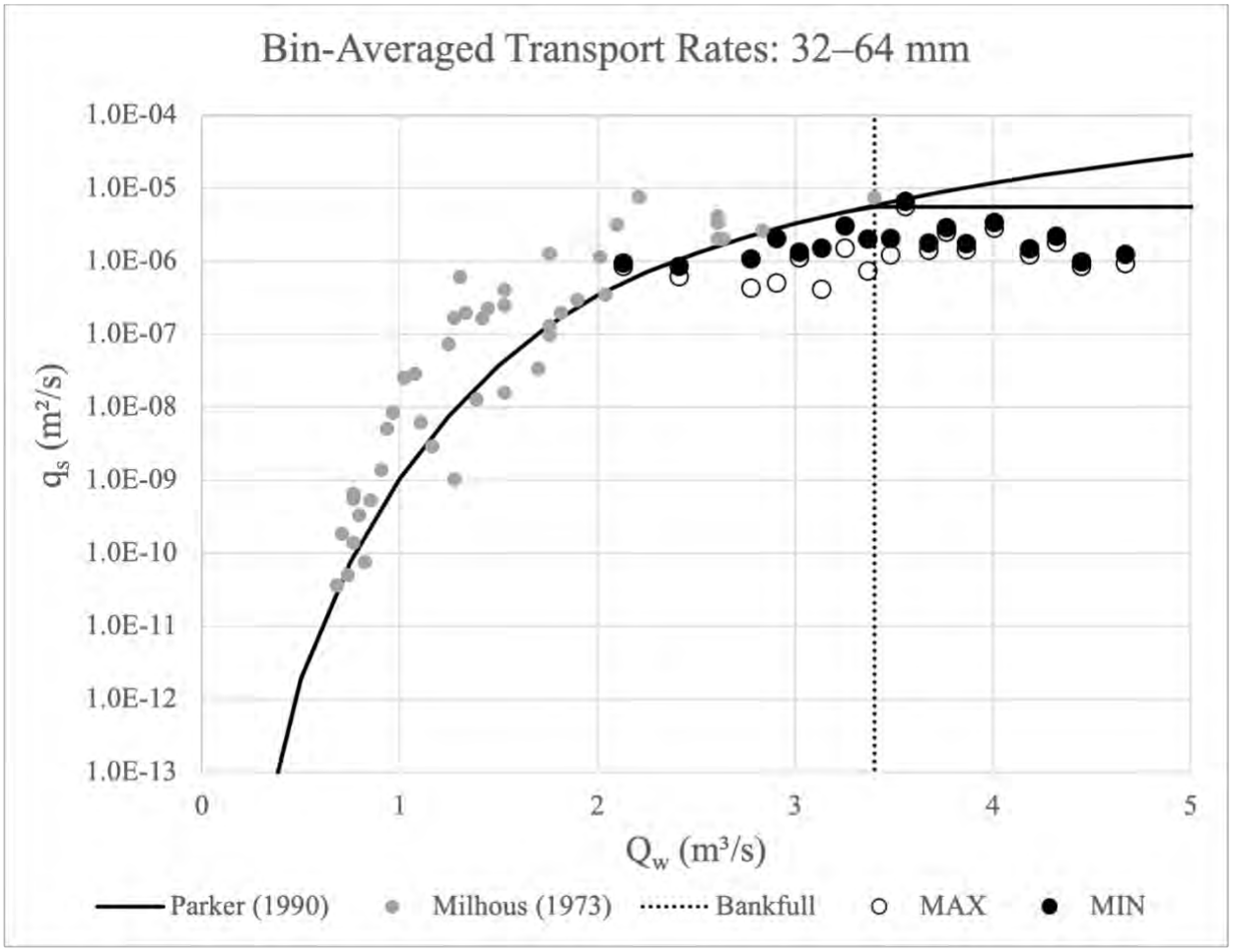

Figure 4.6. Bin averaged transport rates, from 32-64 mm size class, for estimated minimum (solid dots) and maximum (empty dots) transport rate values. Transport rates, q_s, are plotted against the related discharge, Q_w, for each bin and bins consists of ten samples. Solid black line is estimated transport rate for the grain size class based on the Parker (1990) model output and grey dots are data from vortex sampler (Milhous, 1973) used to calibrate the Parker model. The second, lower, Parker model output at higher discharges was leveled off to show bankfull conditions and the vertical, dotted line at 3.4 m^3/s displays the discharge at bankfull conditions. Y-axis is plotted in log scale.

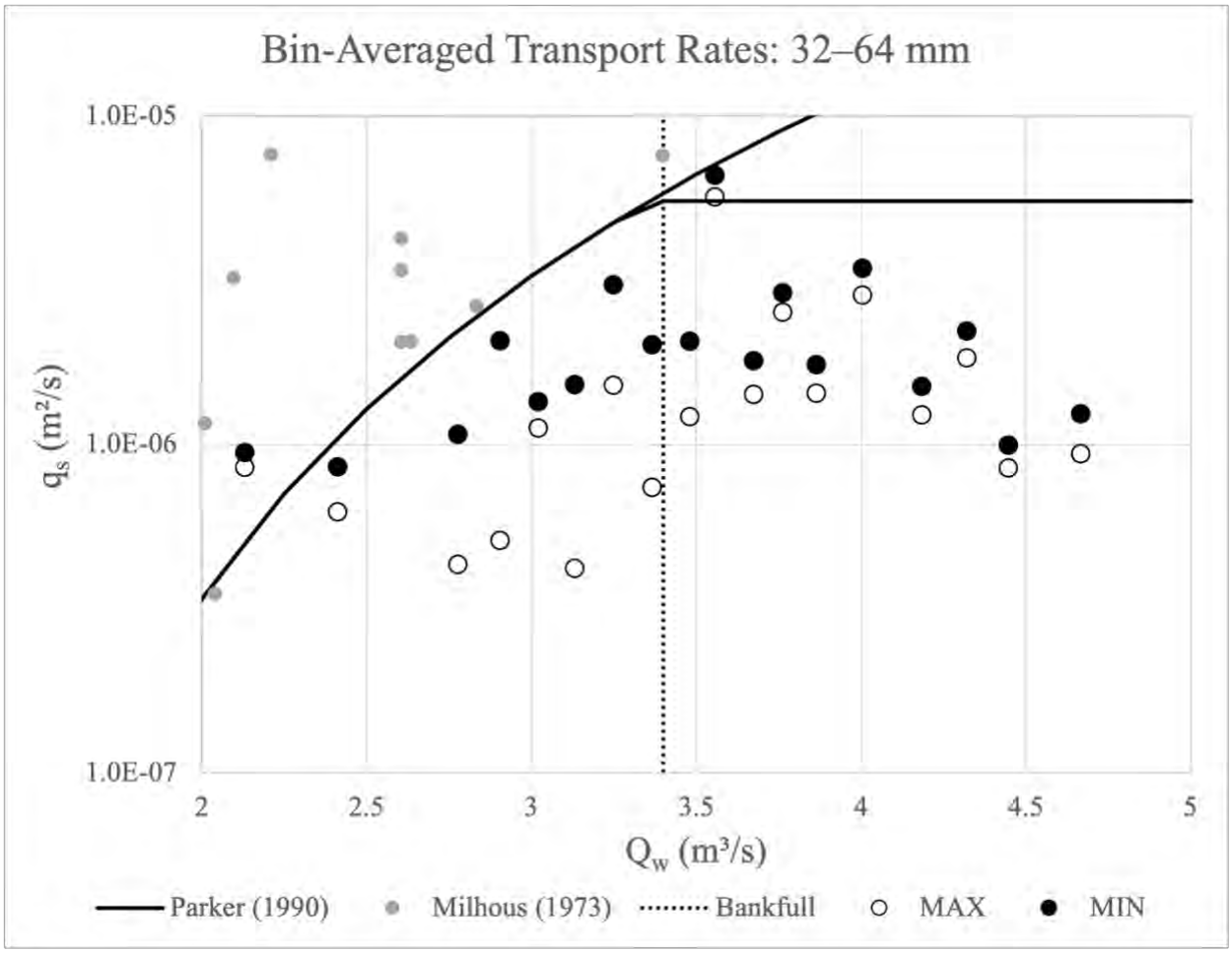

Figure 4.7. Same data and graph as Figure 4.6 but zoomed in on the bin-averaged transport rates from this study to show any trends between data points.

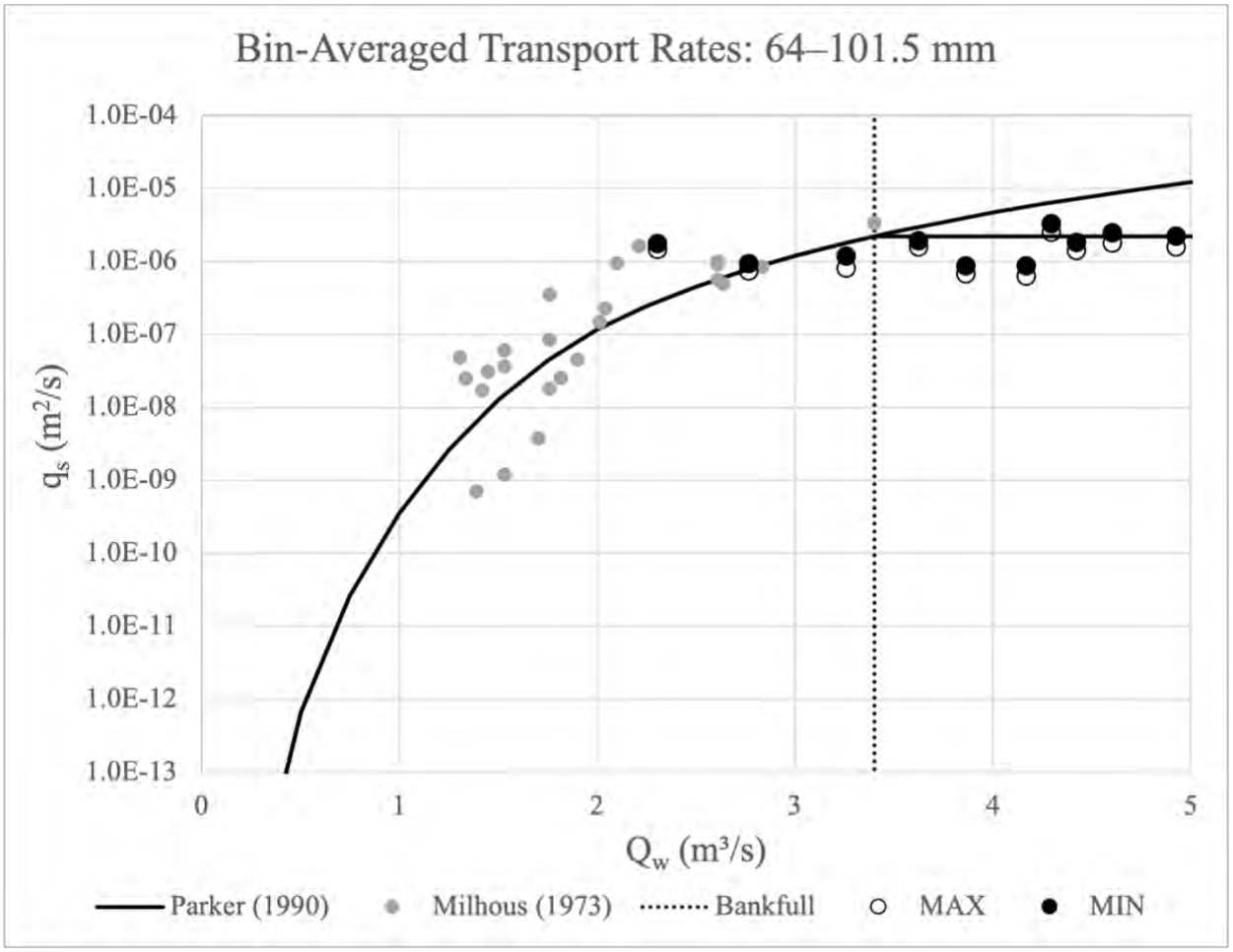

Figure 4.8. Bin averaged transport rates, from 64-101.5 mm size class, for estimated minimum (solid dots) and maximum (empty dots) transport rate values. Transport rates, q_s, are plotted against the related discharge, Q_w, for each bin and bins consists of ten samples. Solid black line is estimated transport rate for the grain size class based on the Parker (1990) model output and grey dots are data from vortex sampler (Milhous, 1973) used to calibrate the Parker model. The second, lower, Parker model output at higher discharges was leveled off to show bankfull conditions and the vertical, dotted line at 3.4 m^3/s displays the discharge at bankfull conditions. Y-axis is plotted in log scale.

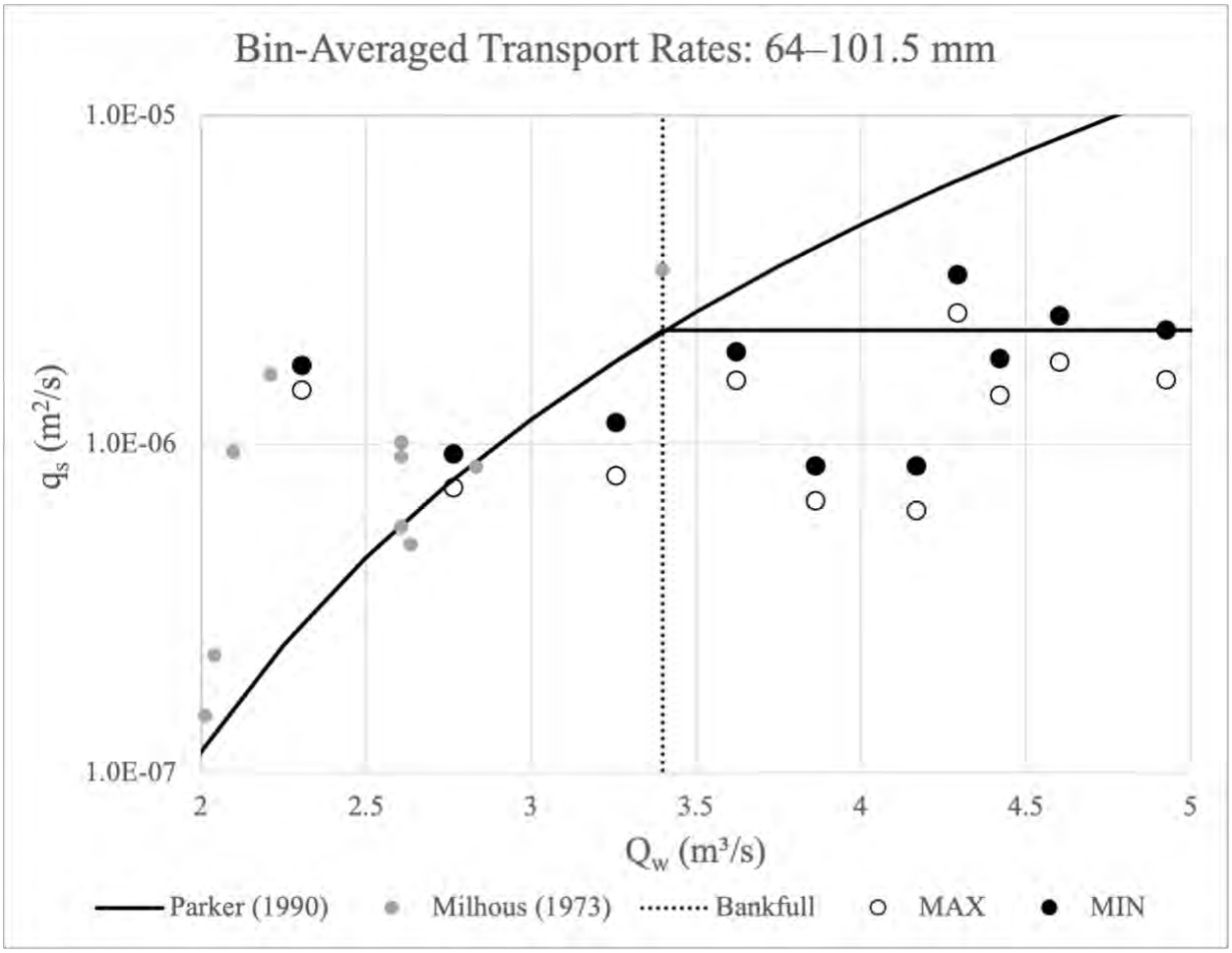

Figure 4.9. Same data and graph as Figure 4.8 but zoomed in on the bin-averaged transport rates from this study to show any trends between data points.

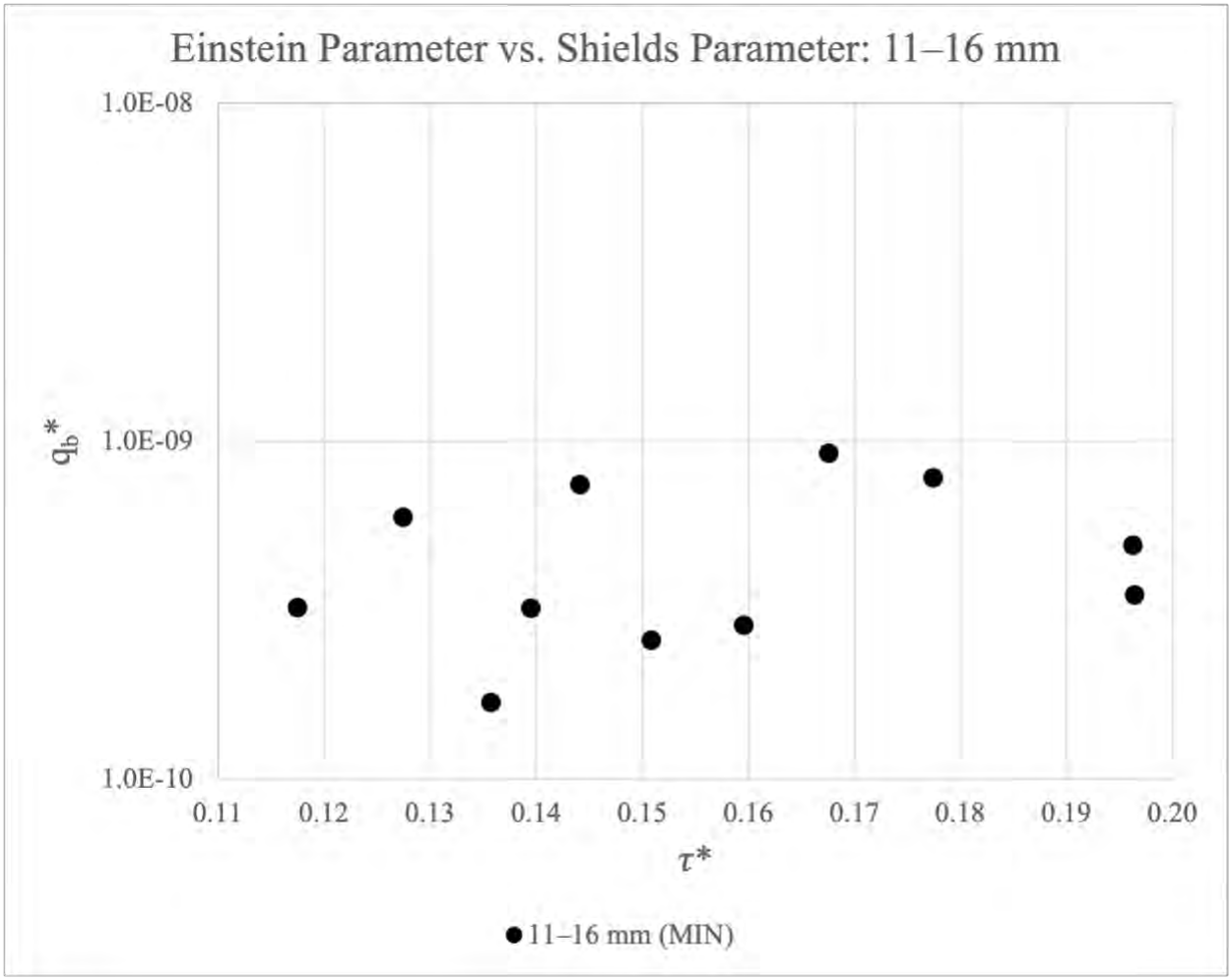

Figure 4.10. Nondimensionalized Einstein parameter plotted against estimated Shields stress for minimum bin-averaged transport rates for all 11–16 mm size class.

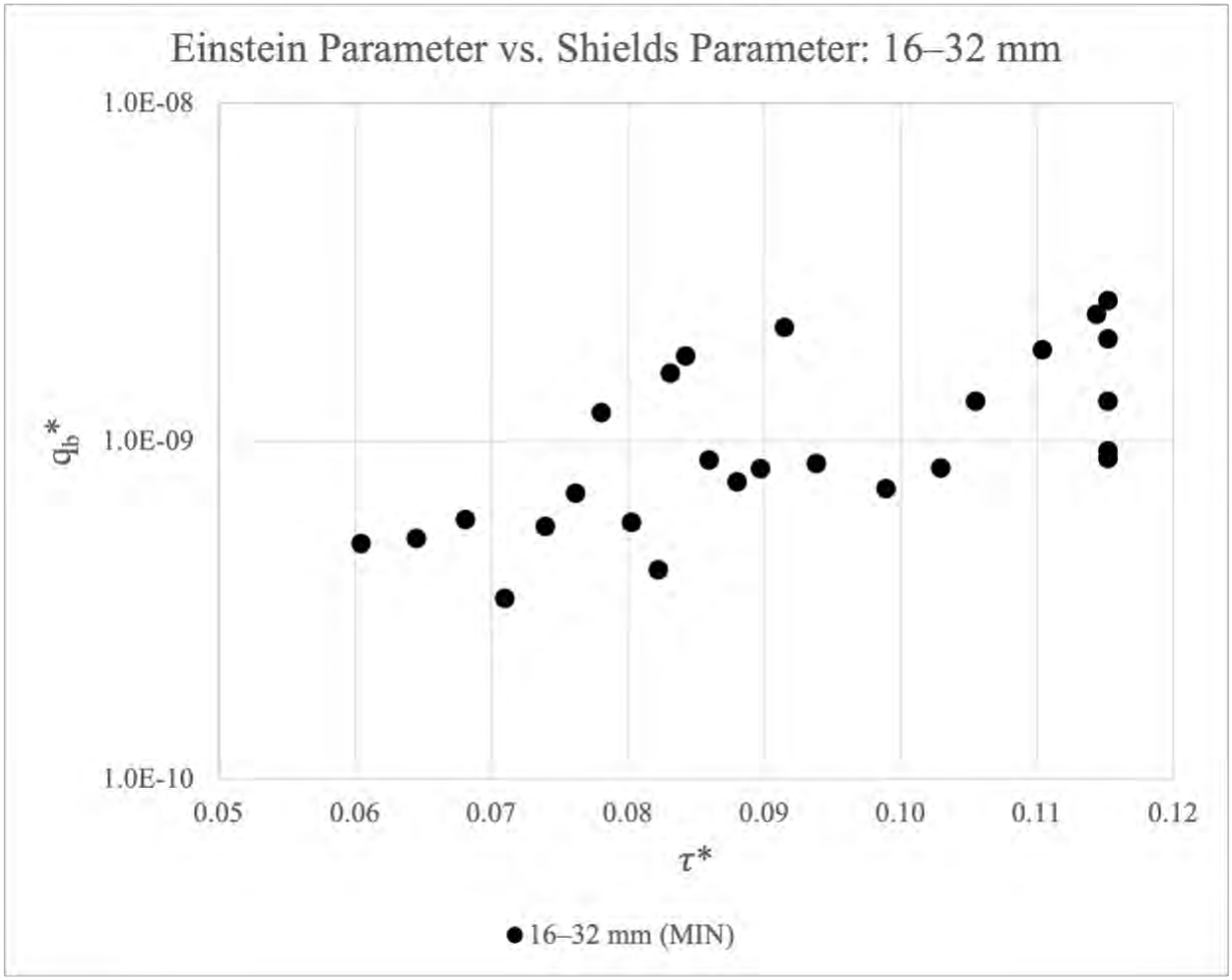

Figure 4.11. Nondimensionalized Einstein parameter plotted against estimated Shields stress for minimum bin-averaged transport rates for all 16–32 mm size class.

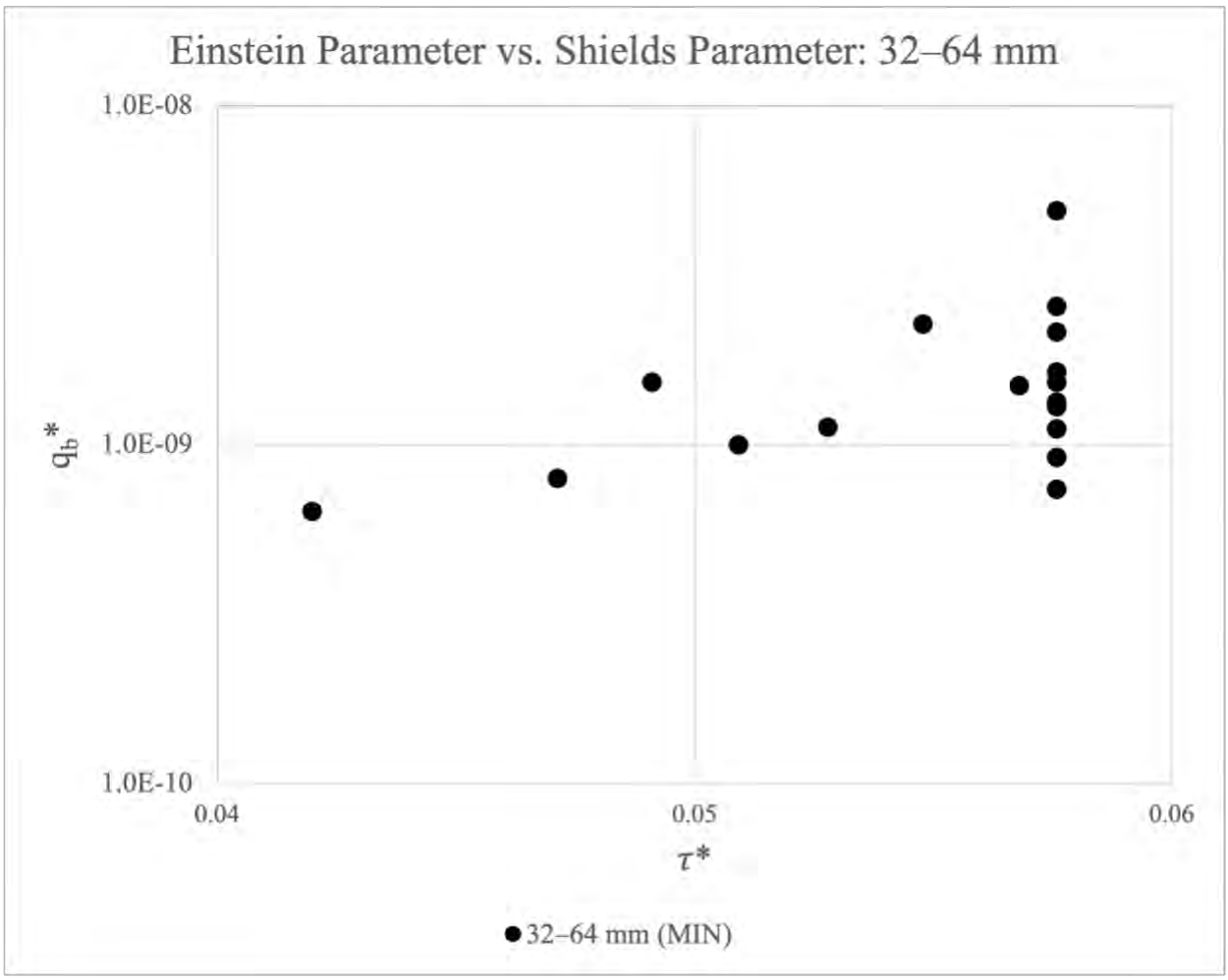

Figure 4.12. Nondimensionalized Einstein parameter plotted against estimated Shields stress for minimum bin-averaged transport rates for all 32–64 mm size class.

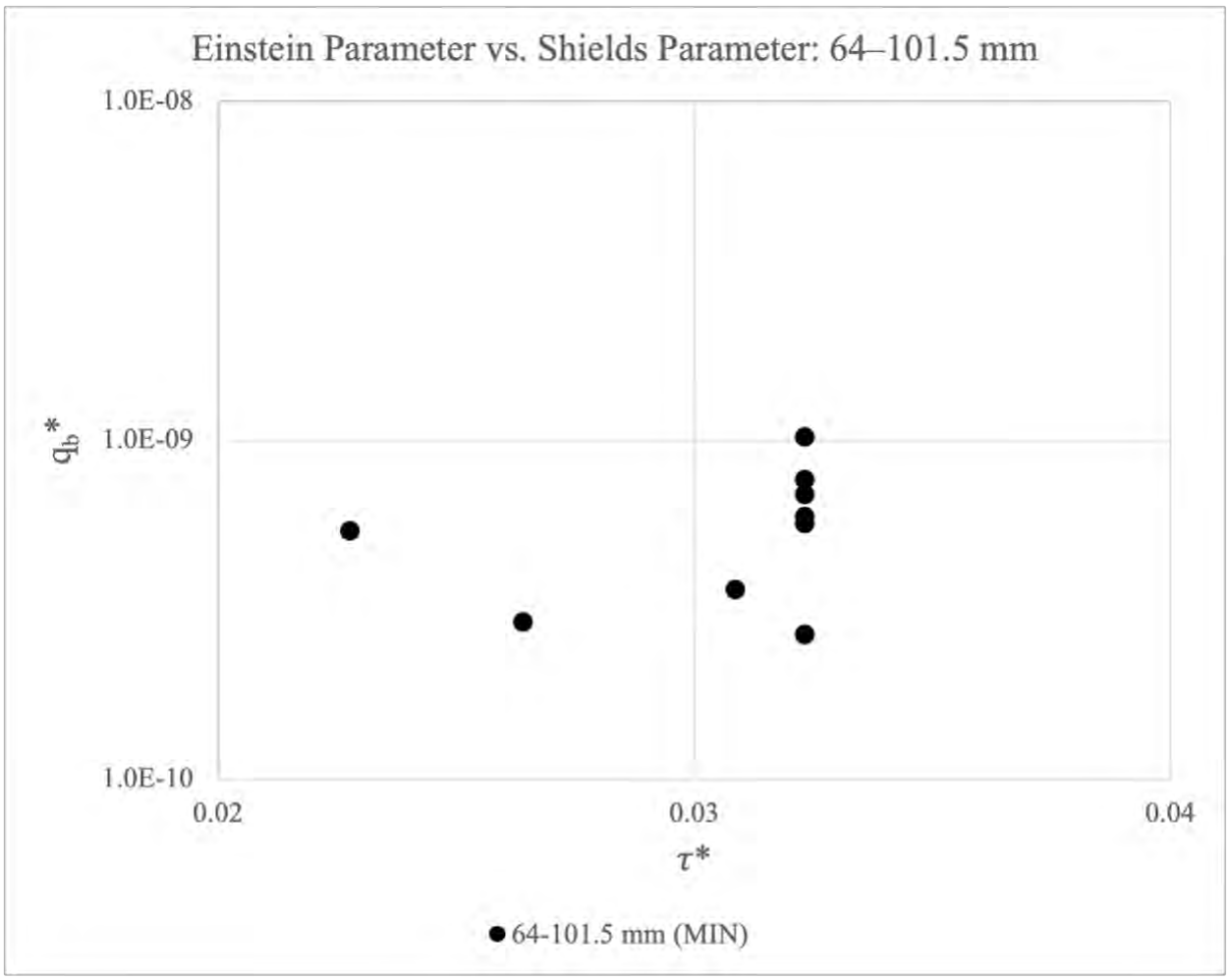

Figure 4.13. Nondimensionalized Einstein parameter plotted against estimated Shields stress for minimum bin-averaged transport rates for all 64–101.5 mm size class.

5 Discussion:

5.1 Tracer and RFID System

Several problems and complications using the method presented themselves over the course of the study that limited the ability to collect data, but problems with the system did not affect the quality of the data gathered. First, large tracers could become immobile near an antenna and effectively hide all other tracers that would move past an antenna. This occurred because an antenna can only identify one tracer particle at a time in its readable range. Additionally, the two larger size classes from the initial deployment were tagged with larger PIT tags, so those tracers were able to be detected from a slightly larger range and if immobile near an antenna, could more effectively block the passage of tracers with the smaller tags. The combination of those complications made the detection of smaller tracers, and all tracers, less likely to occur at times of transport. If no tracers would have become immobile near an antenna, more inter-arrival times could have been gathered and less tracers could have traveled through the array without being detected.

Due to a significant number of tracers moving through the system without being detected, minimum and maximum values for transport were generated and could differ widely from each other. As presented in the results, differences in maximum and minimum values for the smaller size class could differ by over an order of magnitude. These large ranges are likely due to immobile tracers blocking detections at an antenna and from the large transport distances associate with particles of the smaller size class. If a tracer moving out of the antenna array was

not identified by the last antenna, mobile tracking detection downstream of the last antenna was required to effectively categorize a tracer as out of the system, so unable to be on the surface of the bed in the study area reach. Early mobile tracking efforts, from 2016-2019, allowed for the entire stream bed to be monitored for over 2,000 meters downstream of the last antenna, while efforts after 2019 only allowed for the stream to be monitored closer to 800 meters downstream of the last antenna. Later limitations to the ability to access the stream at points well downstream of the last antenna for mobile tracking effectively decreased the ability to identify tracers that moved large distances downstream without being detected by the last antenna, or any antennas for that matter.

While a substantial number of tracers from the two smaller class sizes were never detected by the antenna array or mobile tracking, recovery rates from 2016-2019 ranged between 50-70% for the first deployment. Recovery rates for the larger two classes were much higher and ranged between 80-95% for the initial deployment. Later deployments, where mobile tracking was limited, were not as effective and recovery rates for the two smaller size classes were significantly lower, ranging between 30-60%. Lower recovered rates resulted in larger differences between the minimum and maximum calculated transport rates. Rates for later deployments are much lower and not comparable to recent studies using PIT tags, specifically Bradley and Tucker (2012) who reported recovery rates over 90%, like that of the initial deployment. The range of recovery rates from this study more closely match rates identified by Liébault et al. (2012), who found that rates declined from 80% to 30% over a three-year period of monitoring tracers.

To reduce the uncertainty in the number of tracers left in the system and on the surface of the bed, it is likely that utilizing the same size PIT tags on all grain sizes could have reduced the number of tracers moving past antennas without detection. The antennas were stretched across the length of the stream and when initially placed in the stream, they were intended to not disrupt flow or tracers that would have moved past. During visits to the site to turn on the antenna array, antenna locations were inspected to ensure quality of the system and almost always needed to be cleared of leaves and minor woody debris. It is possible that tracers could have been caught in debris during transport and became immobile near an antenna. From looking at antenna records, it was easy to determine when a tracer was immobile for long periods, but without high resolution mobile antennas, it was not possible to locate and move specific tracers immobile near an antenna. Attempting to find specific tracers near an antenna would also disturb the bed and possibly disturb other tracers or transport near an antenna.

It is possible that modifications to the antenna system could have helped to inhibit tracers from stopping next to them, but exactly what type of modifications are not totally clear. Instead of antennas being on the bed of the stream, it is possible to imagine antennas being raised above the bed where tracers and other bed material would not encounter it. Since antennas were secured to the bed with soil anchors, antennas not deployed to the bed would need a different way to ensure safety of the equipment. Large debris would often move over the top of antennas secured to the bed, but an antenna above the bed would likely be significantly harmed by similar debris. Instead of changing the position of the antenna, it is possible that plastic, or another hard and pliable material, could have been placed under the antenna to help bed material move past each antenna. Since tracers moving past the antenna were already assumed to be in motion, assisting movement

would not significantly affect transport in this instance. Even with a smoother material under an antenna, it is still likely that bed material and debris could have been caught by the antennas.

In addition to modifications of the antennas, the placement of more antennas to the antenna array system could have created higher chances of detecting tracers that moved through the system without detection. Since the array system only covered about ~150 meters, extending the array to cover a larger stream length could have added further aid to detecting tracers. In theory, the addition of a larger array system and more antennas seems like an easy solution but getting the array system to work with just three antennas was often difficult. Specifically, ensuring power to all antennas was adequate was a constant component of keeping the system running smoothly. Adding more antennas to the system would have made this task even harder with an already finicky system. More antennas would also mean more wires running through the stream reach and adding more complications to the study area and the reader box components itself. Even at one point with the three-antenna configuration, one of the cables stretching from the reader box to an antenna was presumably eaten through by wildlife and needed to be replaced. Though it is quite likely additions and modifications to the system could have resulted in more tracer detections, the correct steps forward and methods are not entirely clear.

The passage of tracers through the antenna array was assumed to be a Poisson process where the distribution of inter-arrival times is exponentially distributed. This assumption was used to determine outlier detections where either the inter-arrival time was too large or the concentration of tracers on the surface was too low. For all data points, the distribution of inter-arrival times multiplied by the tracer concentration is not exponentially distributed, but instead exhibits a

heavy tail and trend closer to a power law function (Figure 5.1). Once outlier detections were removed, the data is exponentially distributed and agrees with the Poisson process. Since the distribution is dependent on two variables that change with time, a definitive maximum inter-arrival time or tracer concentration cannot be concluded, but generally, inter-arrival times over 12 hours are likely to produce outlier data independent of the tracer concentration. Figure 5.1 only considers one size class of deployed tracers, so results are under the assumption that the distribution of inter-arrival times for other tracers are similar.

5.2 Transport Rates

Overall, the smaller two tracer size classes overwhelmingly undershot the Parker surface-based model (1990), while the larger two size classes resulted in transport rates similar to what was expected. This result was puzzling at first, but a likely problem might be found in the style of tracer deployments. For the first deployment, tracers were deployed over a short distance and were attempted to simulate three different masses of tracers (see Figure 3.12) that would move through the system equally to keep concentrations at a constant rate. Instead of moving through the system equally, tracer positions almost immediately lost the deployment shape, and many moved quickly through the system and hundreds of meters downstream of the last antenna. Simply modifying the study area reach to something larger, from 150 meters to 500 meters, with the transport formulation used for this study, would results in transport rates much higher than what were calculated. This would also result in transport rates that were much closer to the estimated model for the smaller two tracer size classes and resulted in rates above well above the estimated model for the larger size classes. So, it seems that the deployment style for the larger

class sizes were done properly but the smaller classes needed to be deployed over a larger distance due to the large transport distances associated with them. Additionally, evaluating the distance tracers travel to reach an antenna could tell us more about the appropriate study area length and concentration values. Figure 5.2 shows the transport distances tracers traveled to reach an antenna position for deployment 2B over a few months. Potentially, travel distances could be weighted to come to a more accurate study areas instead of the entire length of bed where tracers are on the surface. Changing the study area configuration could represent the concentration of tracers moving through the antenna array more accurately. The differences between the maximum transport distances to reach the three antennas can also be seen in Figure 5.2. Points before the gap in data near 30 m represent tracers that were close to antennas, while later gaps in data near 300 m and 350 m represents the longest distances traveled to reach antennas 1 and 2. The farthest distances traveled define the maximum distance tracers covered to reach the last antenna, antenna 3.

Because of the tracer gravel's ability to move so quickly through the system once introduced to the bed of the stream, later deployments were styled differently as a constant number of tracers over a much larger study area distance and in larger quantities. Even though the later deployments were done so over a larger distance and higher quantity, it seems the concentration of tracers moving through the array at any given point were often too low to be amenable to the method. This means that interarrival times were sometimes too large to be reliably used in the transport formulation. While attempting to solve the problem of tracers not deployed over a large enough distance, not enough tracers were deployed over the extended distance to keep the concentration of tracers moving through the array high enough, again likely resulting in transport

rates too low. While disappointing for this study, it is valuable information of any tracer studies in the future that wishes to use a similar methodology. It is also possible that changes to the deployment style could have had no effects on the calculated transport rates and the leveling off of transport rates at higher discharges is occurring sooner than what is estimated from the Parker (1990) model. Even though results from the larger two size classes match the model more closely than the smaller particle sizes, they still overall undershoot expected rates.

In addition to the two discussed deployment styles, a third style for deployment 3 was used in which tracers were tossed into the stream, just upstream of the two most downstream antennas, during a high discharge event with the hopes of easily gathering detections and generating inter-arrival times. Of the 44 tracers deployed, a total of five antenna detections were recorded and no reliable inter-arrival times were generated. This was a disappointing outcome to a deployment where it was assumed inter-arrival times would be easy to determine with tracer position near antennas and transport of bedload occurring. From mobile tracking records, it was found that many of the tracers moved past antenna during the high flow event in which they were deployed during, and many moved through the entire array system. Due to lack of inter-arrival times, tracer concentrations were not evaluated, and no results were produced from deployment 3.

Another potential problem with the calculated transport rates from this study is the usage of discharges estimated above bankfull. Bankfull conditions for the study reach were previously identified at 3.4 m^3/s (Katz, 2018; Milhous 1973), even though the stage-discharge relationship for this study reliably identified discharges close to 4 m^3/s in the weir, which acts as a perfect rectangular channel for flow. Perhaps, pulling those larger discharge data points back to bankfull

could result in data that is more reliable for the study reach and for comparison with the Parker (1990) surface-based model. Doing this with the data still well undershoots the estimated model for the smaller size classes but is a very close match for the larger particle sizes. Still, it seems either the method for the deployment of smaller particles is not correct, or potentially the expected models need modifications.

Results from this study also indicate that the tracer method is not efficient at producing data at the low end of transport and discharge, compared to that of the Milhous (1973) data. The vortex sampler used to collect previous bedload data was able to sample data for extended times periods compared to that of the tracer method, which relied on high discharges that would move particles significant distances and to produce inter-arrival times small enough to be reliable for the transport formulation. In addition to longer collection periods, the vortex sampler was able to collect a wider range of bedload data, while the tracer method required size classes that were large enough to house PIT tags.

5.3 Broader Impacts

Bedload transport estimates using tracers have been relatively short in timescale and with small numbers of tracers, compared to the number of studies using tracers and the number of studies evaluating the mechanisms of bedload transport. Tracer studies attempting to resolve rates of bedload transport have been limited by the quality of information on particle entrainment, velocity, travel distances, virtual velocity, and depth of the active layer. Specifically, previous studies have attempted to estimate sediment transport based on the continuity of moving bedload

particles (Sekine and Kikkawa, 1992; Wiberg and Dungan 1989), conservation relations (Wilcock and McArdell, 1997), and conservation relations with virtual velocity (Hashchenburger and Church; 1998; Hassan, Church, and Ashworth; 1992; Sayre and Hubbell, 1965). These objectives have been hindered by the ability to estimate thickness of the moving bedload layer, the difficulty to consistently define average step lengths of particles, and the ability to quantify characteristics of particle dispersion during infrequent periods of mobility. The method in this study was able to avoid the limitations presented by other studies attempting to resolve bedload transport rates and likely produces more robust and reliable data than has been presented from similar styles of work.

Other than generating bedload transport rates from a new method and comparing the results to accepted formulations for transport, this study attempted to supply data that could be used by future researchers to evaluate other mechanisms for characterizing and predicting sediment transport in gravel-bed streams. Specifically, empirical relations to estimate mean travel distances have been developed, but parameters of the step-length and resting-time distributions for differing channel morphologies, bed compositions, and flow conditions remains an open topic for research. This study presents an extended history of tracer travel distances separated by specified times of immobility, which could be helpful for evaluating the previous mentioned objectives. From other field observations of tracers, it has been shown that the mean travel distance of particles during high flood events tend to decrease with an increase in particles size (Church and Hassan, 1992; Philips and Jerolamack, 2014). This idea is clearly illustrated in Figure 3.11, and additional results could lend added information to the objective of relating transport distances during floods to different particle sizes.

Nikora et al. (2001) introduced three ranges of spatial and temporal scale of sediment particle motion and the characteristics of particle dispersion at each scale, but few studies have been able to evaluate multiple scales due to the limited length of tracer studies. The first and shortest scale of motion is called the local range and is defined as a particle saltating or rolling in motion along the bed. The second is described as the intermediate ranges and is defined as a series of particle steps followed by a rest period that is longer than that of the time it was in motion. Movements of the intermediate range have been characterized as a series of 18 consecutive saltations by Seminarara, Solari, and Parker (2002), differing from the single saltation represented by the local range. The final and longest scale is the global range and consists of multiple particle movements of the intermediate range separated by significantly longer periods of rest, where periods of rest are more related to flood frequency and storage of particles in bars and riffles. Results from this study may not be fine enough in resolution to resolve the described local and intermediate ranges but can likely help build on motion of the global scale. Particularly, long term records of tracers have several characterized periods of movement that are separated by periods where particles are immobile, presumably locked away in gravels bars or large pools.

It is not yet clear if the PIT tagged tracer method using RFID antennas is yet suitable for use on larger stream system due to the lack of the ability to mobile track and find tracers locations throughout a study area or to locate tracers that may pass an antenna without detection. On a larger stream, it would also be harder to construct an antenna system that could withstand larger discharges. The likelihood of particles becoming buried or immobile near an antenna could also be greater. The prediction of gravel movement in streams of all sizes is an important issue to scientists, engineers, and other related managers who are concerned with the distribution of

particle transport distances and how they relate to overall bedload transport rates. Recent studies by Furbish et al. (2012) and Roseberry et al. (2013) have highlighted the transport of tracer particles once they are deployed to the bed of a stream. Results from this study indicate that once a tracer particle is introduced to a stream, it has a very high likelihood of quickly moving large distances downstream. This is an important finding because a supply of gravel is required for the spawning and rearing of fish in gravel-bed streams, so having better tools to predict how gravel might move when introduced to a stream could improve restoration practices.

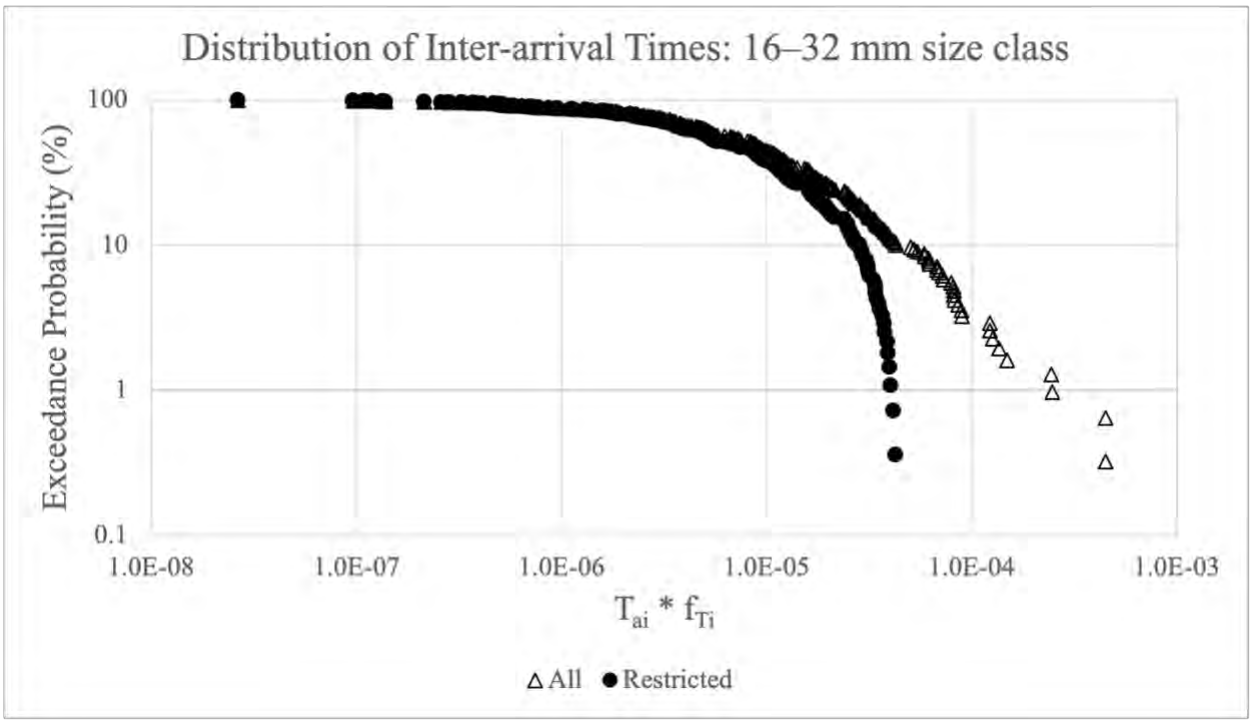

Figure 5.1. Exceedance probability of the distribution of inter-arrival times, T_{ai}, multiplied by the tracer concentration, f_{Ti}, for inter-arrival times from the 16–32 mm size class. The trend for all data points is closer to a power law function and when outlier data are removed, data points are exponentially distributed. Both axes are plotted in log scale.

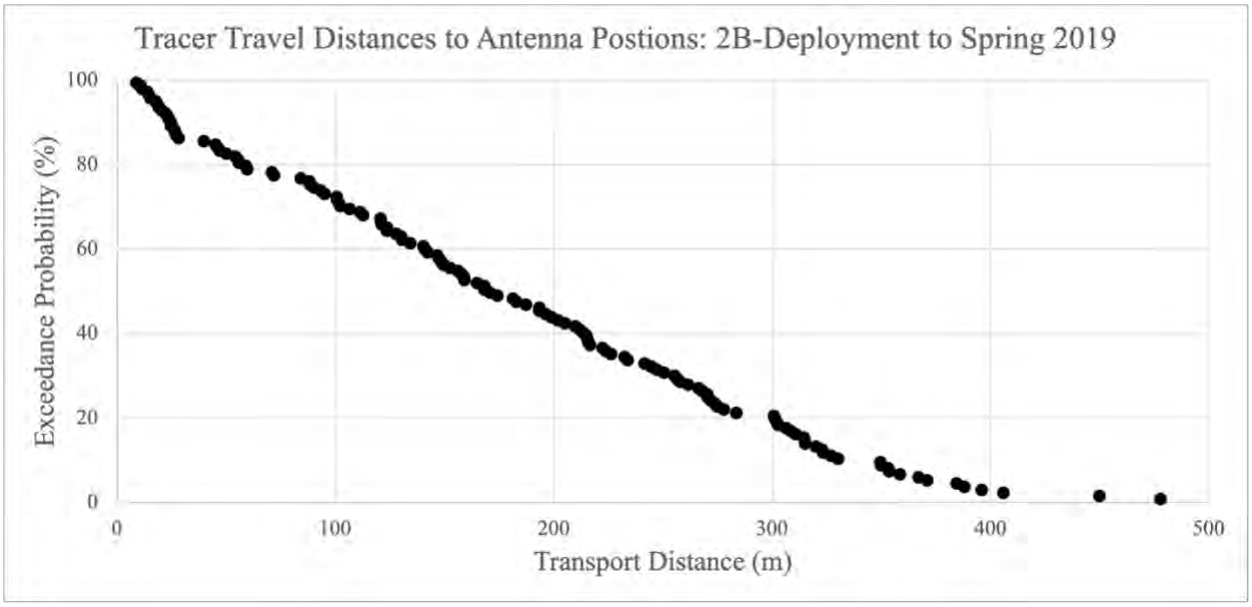

Figure 5.2. Exceedance probability of transport distances for a tracer to reach an antenna position. Plotted data is from deployment 2B over the course of all transport events in a single water year.

6 Conclusion

The primary objective of the study was to determine bedload transport rates using tracer gravel and RFID instrumentation that could be compared with an existing model for Oak Creek, and this primary objective has been accomplished. An additional objective of this study was to leave behind a large database of tracer particle movement that could be utilized by future researchers, and this has also been successfully achieved.

The main conclusion of the research is that the tracer and RFID antenna methodology is effective at monitoring bedload movement and can produce reliable data to be used to formulate transport rates. Close to 3,000 tracer particles were deployed at Oak Creek and monitored between 2016 and 2022 and 685 inter-arrival time samples were recorded to generate transport rates. For the two smaller size classes of tracers, bin-averaged transport rates were an order of magnitude, or more, lower than what was expected from the model for the reach. For the two larger size classes, bin-averaged transport rates were inside an order of magnitude difference from the expected transport model. In all, transport rates for all class sizes were lower than what is expected for the study reach.

The most important aspect for determining transport rates in this study was estimating the number of tracers on the surface of the bed for calculating tracer concentrations for each individual deployment. Due to limitations of the system, tracers could move through the antenna array without being detected and tracers could evade mobile tracking efforts by traveling large distance downstream and out of the reach that was extensively monitored. The primary reason

tracers could move through the antenna array without detection was because tracers could often be immobile near an antenna, which limited the ability of an antenna to detect other tracers passing by. Early mobile tracking periods allowed for monitoring the stream large distances downstream of the array while later efforts were much more limited, which decreased rates of tracer recovery by a significant margin. Limited mobile tracking distance also decreased the ability to detect tracers that moved through the array without any antenna detections.

Previous studies using tracers have been restricted by the number of particles deployed to a stream and the amount of time to assess the movement of those particles. Recent work using PIT tags and RFID antenna instrumentation have enabled longer monitoring time of gravel movement, but data gathered from other research have not been sufficient to reliably measure sediment transport rates in a wide range of flows with specific dates and times. Methods in this study build on the previous work and allow for the characterization of bedload transport rates with a high resolution of time and discharge.

Predicting gravel movement is important for scientist, engineers, and other related parties who are concerned with sediment sources, the distribution of transport distances, and how they are related to overall transport rates. The research in this thesis improves upon the prediction of gravel movement using tracer particles and details some of the complications that are still present. It is likely that building on the inefficiencies found in this research could allow for the method to be utilized on a larger stream, where data for larger particles and larger flows could be gathered.

Bibliography

Bathurst, J.C., Hey, R.D. and Thorne, C.R. eds., 1987. Sediment transport in gravel-bed rivers (pp. 453-491). Chichester, UK: Wiley.

Bradley, D.N. and Tucker, G.E., 2012. Measuring gravel transport and dispersion in a mountain river using passive radio tracers. *Earth Surface Processes and Landforms*, *37*(10), pp.1034-1045.

Bradley, D.N., 2017. Direct observation of heavy-tailed storage times of bed load tracer particles causing anomalous superdiffusion. *Geophysical Research Letters*, *44*(24), pp.12-227.

Carling, P.A., Williams, J.J., Kelsey, A., Glaister, M.S. and Orr, H.G., 1998. Coarse bedload transport in a mountain river. *Earth Surface Processes and Landforms: The Journal of the British Geomorphological Group*, *23*(2), pp.141-157.

Collins, A.L., Walling, D.E. and Leeks, G.J.L., 1997. Source type ascription for fluvial suspended sediment based on a quantitative composite fingerprinting technique. *Catena*, *29*(1), pp.1-27.

Church, M. and Hassan, M.A., 1992. Size and distance of travel of unconstrained clasts on a streambed. *Water Resources Research*, *28*(1), pp.299-303.

Einstein, H.A., 1950. The bed-load function for sediment transportation in open channel flows (No. 1026). US Government Printing Office.

Ergenzinger, P. and Schmidt, K.H., 1990. Stochastic elements of bed load transport in a step-pool mountain river. *IN: Hydrology of Mountainous Regions--II: Artificial Reservoirs, Water and Slopes. IAHS Publication*, (194).

Furbish, D.J., Haff, P.K., Roseberry, J.C. and Schmeeckle, M.W., 2012. A probabilistic description of the bed load sediment flux: 1. Theory. *Journal of Geophysical Research: Earth Surface*, *117*(F3).

Habersack, H.M., 2001. Radio-tracking gravel particles in a large braided river in New Zealand: A field test of the stochastic theory of bed load transport proposed by Einstein. *Hydrological Processes*, *15*(3), pp.377-391.

Haschenburger, J.K. and Church, M., 1998. Bed material transport estimated from the virtual velocity of sediment. *Earth Surface Processes and Landforms: The Journal of the British Geomorphological Group*, *23*(9), pp.791-808.

Hassan, M.A., Church, M. and Ashworth, P.J., 1992. Virtual rate and mean distance of travel of individual clasts in gravel-bed channels. *Earth Surface Processes and Landforms*, *17*(6), pp.617-627.

Hassan, M.A. and Bradley, D.N., 2017. Geomorphic controls on tracer particle dispersion in gravel-bed rivers. *Gravel-bed rivers: Processes and disasters*, pp.159-184.

Hoey, T., 1992. Temporal variations in bedload transport rates and sediment storage in gravel-bed rivers. *Progress in physical geography*, *16*(3), pp.319-338.

Hubbell, D.W. and Sayre, W.W., 1964. Sand transport studies with radioactive tracers. *Journal of the Hydraulics Division*, *90*(3), pp.39-68.

Hudson, R. and Fraser, J., 2005. The mass balance (or dry injection) method. *Streamline Watershed Management Bulletin*, *9*(1), pp.6-12.

Katz, S.B., Segura, C. and Warren, D.R., 2018. The influence of channel bed disturbance on benthic Chlorophyll a: A high resolution perspective. *Geomorphology*, *305*, pp.141-153.

Lamarre, H., MacVicar, B. and Roy, A.G., 2005. Using passive integrated transponder (PIT) tags to investigate sediment transport in gravel-bed rivers. *Journal of Sedimentary Research*, *75*(4), pp.736-741.

Lamarre, H. and Roy, A.G., 2008. The role of morphology on the displacement of particles in a step–pool river system. *Geomorphology*, *99*(1-4), pp.270-279.

Leopold, L.B. and Emmett, W.W., 1977. 1976 bedload measurements, East Fork River, Wyoming. *Proceedings of the National Academy of Sciences*, *74*(7), pp.2644-2648.

Liedermann, M., Tritthart, M. and Habersack, H., 2013. Particle path characteristics at the large gravel-bed river Danube: results from a tracer study and numerical modelling. *Earth Surface Processes and Landforms*, *38*(5), pp.512-522.

Liébault, F., Bellot, H., Chapuis, M., Klotz, S. and Deschâtres, M., 2012. Bedload tracing in a high-sediment-load mountain stream. *Earth Surface Processes and Landforms*, *37*(4), pp.385-399.

McNamara, J.P. and Borden, C., 2004. Observations on the movement of coarse gravel using implanted motion-sensing radio transmitters. *Hydrological Processes*, *18*(10), pp.1871-1884.

Meyer-Peter, E. and Müller, R., 1948. Formulas for bed-load transport. In *IAHSR 2nd meeting, Stockholm, appendix 2*. IAHR.

Milhous, R. T., 1973. Sediment transport in a gravel-bottomed stream, Ph.D. thesis, Oregon State University, Corvallis, Oregon.

Miller, J.R., Lord, M., Yurkovich, S., Mackin, G. and Kolenbrander, L., 2005. Historical trends in Sedimentation rates and sediment provenance, Fairfield Lake, western North Carolina. *JAWRA Journal of the American Water Resources Association*, *41*(5), pp.1053-1075.

Monsalve, A., Yager, E.M., Turowski, J.M. and Rickenmann, D., 2016. A probabilistic formulation of bed load transport to include spatial variability of flow and surface grain size distributions. *Water Resources Research*, *52*(5), pp.3579-3598.

Monsalve, A., Segura, C., Hucke, N. and Katz, S., 2020. A bed load transport equation based on the spatial distribution of shear stress–Oak Creek revisited. *Earth Surface Dynamics*, *8*(3), pp.825-839.

Nikora, V., Heald, J., Goring, D. and McEwan, I., 2001. Diffusion of saltating particles in unidirectional water flow over a rough granular bed. *Journal of Physics A: Mathematical and General*, *34*(50), p.L743.

Olinde, L. and Johnson, J.P., 2013, December. Characterizing coarse bedload transport during floods with RFID and accelerometer tracers, in-stream RFID antennas and HEC-RAS modeling. In *AGU Fall Meeting Abstracts* (Vol. 2013, pp. EP32B-05).

Olinde, L. and Johnson, J.P., 2015. Using RFID and accelerometer-embedded tracers to measure probabilities of bed load transport, step lengths, and rest times in a mountain stream. *Water Resources Research*, *51*(9), pp.7572-7589

Parker, G. and Klingeman, P.C., 1982. On why gravel bed streams are paved. *Water Resources Research*, *18*(5), pp.1409-1423.

Parker, G., Klingeman, P.C. and McLean, D.G., 1982. Bedload and size distribution in paved gravel-bed streams. *Journal of the Hydraulics Division*, *108*(4), pp.544-571.

Parker, G., 1990. Surface-based bedload transport relation for gravel rivers, *Journal of Hydraulic Research*, 28 (4), 417-436.

Phillips, C.B., Martin, R.L. and Jerolmack, D.J., 2013. Impulse framework for unsteady flows reveals superdiffusive bed load transport. *Geophysical Research Letters*, *40*(7), pp.1328-1333.

Phillips, C.B. and Jerolmack, D.J., 2014. Dynamics and mechanics of bed-load tracer particles. *Earth Surface Dynamics*, *2*(2), pp.513-530.

Recking, A., 2013a. Simple method for calculating reach-averaged bed-load transport. *Journal of Hydraulic Engineering*, *139*(1), pp.70-75.

Recking, A., 2013b. An analysis of nonlinearity effects on bed load transport prediction. *Journal of Geophysical Research: Earth Surface*, *118*(3), pp.1264-1281.

Roseberry, J.C., Schmeeckle, M.W. and Furbish, D.J., 2012. A probabilistic description of the bed load sediment flux: 2. Particle activity and motions. *Journal of Geophysical Research: Earth Surface*, *117*(F3).

Sayre, W.W. and Hubbell, D.W., 1965. *Transport and dispersion of labeled bed material, North Loup River, Nebraska*. US Government Printing Office.

Schmidt, K.H. and Ergenzinger, P., 1992. Bedload entrainment, travel lengths, step lengths, rest periods—studied with passive (iron, magnetic) and active (radio) tracer techniques. *Earth surface processes and landforms*, *17*(2), pp.147-165.

Schneider, J., Hegglin, R., Meier, S., Turowski, J.M., Nitsche, M. and Rickenmann, D., 2010. Studying sediment transport in mountain rivers by mobile and stationary RFID antennas. *River flow 2010*, pp.1723-1730.

Segura, C. and Pitlick, J., 2015. Coupling fluvial-hydraulic models to predict gravel transport in spatially variable flows. *Journal of Geophysical Research: Earth Surface*, *120*(5), pp.834-855.

Sekine, M. and Kikkawa, H., 1992. Mechanics of saltating grains. II. *Journal of Hydraulic Engineering*, *118*(4), pp.536-558.

Seminara, G., Solari, L. and Parker, G., 2002. Bed load at low Shields stress on arbitrarily sloping beds: Failure of the Bagnold hypothesis. *Water resources research*, *38*(11), pp.31-1.

Snavely, P.D., MacLeod, N.S. and Wagner, H.C., 1968. Tholeiitic and alkalic basalts of the Eocene Siletz River volcanics, Oregon coast range. *American Journal of Science*, *266*(6), pp.454-481.

Walling, D.E., Owens, P.N. and Leeks, G.J., 1999. Fingerprinting suspended sediment sources in the catchment of the River Ouse, Yorkshire, UK. *Hydrological processes*, *13*(7), pp.955-975.

Wilcock, P.R. and McArdell, B.W., 1997. Partial transport of a sand/gravel sediment. *Water Resources Research*, *33*(1), pp.235-245.

Williams, G.P., 1989. Sediment concentration versus water discharge during single hydrologic events in rivers. *Journal of Hydrology*, *111*(1-4), pp.89-106.

Wiberg, P.L. and Dungan Smith, J., 1989. Model for calculating bed load transport of sediment. *Journal of hydraulic engineering*, *115*(1), pp.101-123.

Yager, E.M., Dietrich, W.E., Kirchner, J.W. and McArdell, B.W., 2012. Prediction of sediment transport in step-pool channels. *Water Resources Research*, *48*(1).